Leaf Wax Hydrogen Isotopes as a Hydroclimate Proxy in the Tropical Pacific

S. N. Ladd[1,2*], A. E. Maloney[3,4], D. B. Nelson[5], M. Prebble[6,7], G. Camperio[1,2], D. A. Sear[8], J. D. Hassall[8], P. G. Langdon[8], J. P. Sachs[3], and N. Dubois[1,2]

[1]Swiss Federal Institute of Aquatic Science and Technology (EAWAG), Dept. of Surface Waters – Research and Management, Dübendorf, CH. [2]Swiss Federal Institute of Technology (ETH-Zürich), Dept. of Earth Sciences, Zürich, CH. [3]University of Washington, School of Oceanography, Seattle, USA. [4]Princeton University, Dept. of Geosciences, Princeton, USA. [5]University of Basel, Dept. of Environmental Sciences-Botany, Basel, CH. [6]University of Canterbury, School of Earth and Environment, Christchurch, NZ. [7]Australian National University, School of Culture, History and Languages, Canberra, AU. [8]University of Southampton, School of Geography and Environmental Science, Southampton, UK.

Corresponding author: S. Nemiah Ladd (nemiah.ladd@cep.uni-freiburg.de)

*Current address: University of Freiburg, Ecosystem Physiology, Freiburg, DE

Key Points:

- Leaf wax $^{2}H/^{1}H$ ratios are correlated with mean annual precipition $^{2}H/^{1}H$ ratios globally, but not in the tropical Pacific
- Uncertainty in estimates of tropical Pacific precipation $^{2}H/^{1}H$ ratios likely accounts for poor correlations with leaf wax $^{2}H/^{1}H$ ratios
- Palynological analyses indicate that there are no clear relationships between plant community and deviations from the global relationship

Abstract

The hydrogen isotope composition ($^2H/^1H$ ratios) of leaf waxes preserved in sediments is increasingly used to reconstruct past hydroclimate. Here, we extend the global calibration of leaf wax $^2H/^1H$ ratios to include surface sediments from 23 lakes and swamps on 15 tropical Pacific islands. Leaf wax $^2H/^1H$ ratios from this new data set are not correlated with regional estimates of mean annual precipitation $^2H/^1H$ ratios derived from isoscapes or from isotope-enabled general circulation models. Nevertheless, the new data fall within the predicted range of values based on a global calibration compiled from published surface sediments. In our global compilation, we find a strong positive linear correlation between $^2H/^1H$ ratios of mean annual precipitation and the common leaf waxes *n*-C_{29}-alkane ($R^2 = 0.73$, n = 581) and *n*-C_{28}-acid ($R^2 = 0.74$, n = 242). In the tropical Pacific, the largest residuals are no greater than those observed elsewhere, and are likely due to (1) uncertainty in the $^2H/^1H$ ratios of local precipitation and (2) variability in net fractionation for different plant types. Palynological analyses from the same samples suggest that there is no systematic relationship between any particular type of pollen distribution and deviations from the global calibration line. Overall, our results support the use of leaf wax $^2H/^1H$ ratios in tropical Pacific lake sediments as proxies for large hydrological changes, especially when paired with $^2H/^1H$ ratios of source-specific biomarkers. However, the interpretation of such records needs to be informed by careful consideration of local drivers of precipitation isotope variability.

Plain Language Summary

Precipitation is difficult to reconstruct in the past, limiting our ability to understand Earth's climate system. Geochemists learn about past precipitation by measuring the amount of heavy hydrogen incorporated into the waxy coating of leaves, which is preserved in mud that

accumulates in lakes and oceans. Calibration studies have shown that heavy hydrogen in leaf waxes is strongly correlated with heavy hydrogen in local precipitation, allowing us to learn about rainfall intensity, temperature, and cloud movement. However, none of these calibration studies include sites from the tropical Pacific, home of some of the most intense rainfall on the planet and local island populations that rely on that rain for drinking water. We measured heavy hydrogen in leaf waxes from islands throughout the tropical Pacific and show that the values are what we expect based on the global calibration. However, there is no local relationship with precipitation. The types of plants do not explain the lack of correlation, which is more likely due to limitations in the estimates of heavy hydrogen in local rain. Heavy hydrogen from ancient leaf waxes in tropical Pacific mud can show big changes in past precipitation, but smaller changes will not be clear with this tool.

1 Introduction

As Earth warms, precipitation intensity, frequency, and spatial distribution are expected to change over the tropical Pacific (Brown et al., 2011; Tan et al., 2015; Sharmila et al., 2018). These predictions need to be constrained and validated by robust reconstructions of past changes. Unfortunately, there is limited information about past precipitation changes in the western tropical Pacific, in part because of a lack of suitable proxies and archives for producing high resolution, continuous records (Hassall 2017). Existing high-resolution paleohydrologic records from the western tropical Pacific have been established from speleothems (Partin et al., 2013; Maupin et al., 2014) and corals (Quinn et al., 1993; Quinn et al., 1998; Hendy et al, 2002; Linsley et al., 2004; Linsley et al., 2006; Calvo et al., 2007; DeLong et al., 2012), but are generally limited to the past 600 years in this region. Lacustrine and swamp sediments offer the opportunity for longer records of much higher resolution than are possible from slowly

accumulating marine sediments. Lakes and swamps have long been established as archives of ecological, anthropogenic, and broad climatic changes in the region (Southern, 1986; Hope and Pask, 1998; Stevenson et al., 2001; Prebble and Wilmshurst, 2009; Prebble et al., 2019; Gosling et al., 2020). More recently, such sediments have also been used to reconstruct past hydroclimate change in the western tropical Pacific at higher temporal resolution (Sachs et al., 2009; Smittenburg et al., 2011; Konecky et al., 2016; Richey & Sachs, 2016; Hassall, 2017; Sachs et al., 2018; Sear et al., 2020).

One hydroclimate proxy suitable for tropical lake and swamp sediments in the tropical Pacific is based on the hydrogen isotopic composition of leaf waxes (δ^2H_{Wax}= ($^2H/^1H_{Wax}$)/($^2H/^1H_{VSMOW}$) − 1) (Sachse et al., 2012; Konecky et al., 2016; Hassall, 2017). δ^2H_{Wax} values are highly correlated with hydrogen isotopes of mean annual precipitation (δ^2H_P) on a global scale and have been applied to reconstruct δ^2H_P values in diverse locations (Sachse et al., 2012; McFarlin et al., 2019). δ^2H_P values are related to specific physical processes and can be modeled in modern systems with increasing accuracy, making their reconstructions useful for understanding past hydroclimate dynamics (Bowen et al., 2019).

As is typical for organic geochemical proxies, the relationship between δ^2H_{Wax} and δ^2H_P has been established through core-top calibrations with surface sediments from lakes and surface soils. These calibration efforts began in Europe (Sachse et al., 2004; Leider et al., 2013; Nelson et al., 2018) and have been extended to the Americas (Hou et al., 2008; Polissar and Freeman, 2010; Douglas et al., 2013; Nelson, 2013; Shanahan et al., 2013; Bakkelund et al., 2018; Freimuth et al., 2020), East Asia and the Tibetan Plateau (Jia et al., 2008; Aichner et al., 2010; Bai et al., 2011; Wang et al., 2017; Li et al., 2019), and Africa (Peterse et al., 2009; Garcin et al., 2012; Schwab et al, 2015; Herrmann et al., 2017; Jaeschke et al., 2018) (Figure 1). However, the

relationship between δ^2H_{Wax} and δ^2H_P has not yet been assessed on a regional scale in the tropical Pacific.

Two considerations make it particularly important to include regional data in the global calibration before applying it to the tropical Pacific. Firstly, different vegetation types can influence net community fractionation between mean annual precipitation and leaf waxes. Net fractionation between precipitation and leaf waxes is typically expressed by the fractionation factor $\alpha_{Wax\text{-}P}$ ($\alpha_{Wax\text{-}P} = (^2H/^1H)_{Wax}/(^2H/^1H)_P$) or as the enrichment factor $\varepsilon_{Wax\text{-}P} = (\alpha_{Wax\text{-}P} - 1)$ It is well established that $\alpha_{Wax\text{-}P}$ is not constant among plant types or environments (Feakins and Sessions, 2010; Sachse et al., 2012; Kahmen et al., 2013). The unique plant communities on tropical Pacific islands include many endemic species (Gillespie et al., 2013), thus meriting their own regional calibration. Additionally, coastal regions or former lagoons on these islands are often covered by mangrove swamps, which consist of trees and shrubs adapted to brackish to hypersaline water. Higher salinity is correlated with lower $\alpha_{Wax\text{-}P}$ values in mangroves, meaning that their δ^2H_{Wax} values may respond in the opposite way to changes in precipitation intensity to those expected from nearby freshwater plants (Ladd and Sachs, 2012; He et al., 2017; Ladd and Sachs, 2017). However, the impact of mangrove contributions to sedimentary δ^2H_{Wax} values has not previously been assessed.

A second, and perhaps more fundamental consideration, is the uncertainty associated with estimates of δ^2H_P in the tropical Pacific. Direct measurements of δ^2H_P from the global network of isotopes in precipitation (GNIP) are spatially and temporally limited in comparison with other regions. This paucity of data results in large uncertainties for statistical interpolations of δ^2H_P such as that used for the Online Isotopes in Precipitation Calculator (OIPC; Bowen and Revenaugh, 2003). Estimates of δ^2H_P from general circulation models (GCMs) in which

precipitation isotopes have been incorporated offer another potential calibration target for δ^2H_{Wax} measurements in the modern tropical Pacific that to date has not been explored.

Here we measured δ^2H values of 7 *n*-alkane homologues and 5 *n*-alkanoic acid homologues from surface sediments collected from lakes influenced by precipitation from the South Pacific Convergence Zone (SPCZ) and from Micronesian mangrove swamps influenced by the Intertropical Convergence Zone (ITCZ). We add new core-top δ^2H_{Wax} measurements of two of these compounds (*n*-C_{29}-alkane and *n*-C_{28}-acid) from 23 lakes and mangrove swamps on 15 islands distributed throughout the tropical Pacific to a global compilation of δ^2H_{Wax} values. We assess how consistent δ^2H_{Wax} values from tropical Pacific lake and swamp sediments are with the global relationship between δ^2H_{Wax} and modeled δ^2H_P values from a diverse set of algorithms and models. We also compare modeled precipitation δ^2H_P values with each other, with a focus on the tropical Pacific. Finally, we use pollen-based vegetation reconstructions to evaluate the controls that plant communities have on δ^2H_{Wax} values in the tropical Pacific.

2 Materials and Methods

2.1 Site description and sample collection

Surface lake sediments were collected from 19 lakes on 11 islands across the South Pacific Convergence Zone (SPCZ) region of the tropical Pacific (Figure 1, Table 1), ranging in altitude above mean sea level from 790 m (Lanoto'o, Samoa) to 1 m (Rimatu'u, Oroatera, and Onetahi ponds on Tetiaroa, French Polynesia). Lakes ranged from shallow ephemeral water bodies to an 88 m deep volcanic crater lake (Lake Lalolalo, Wallis). The majority of lakes were freshwater systems, but the brackish (salinity = 17) coastal Lake Dranoniveilomo (Fiji) was also included, as well as Lake Lalolalo (Wallis), which is characterized by a freshwater surface lens above saline water at depth (Sichrowsky et al., 2014). Mangrove trees surrounded Lake

Dranoniveilomo, while many other sites were located in forested regions, some of which were impacted by human activity, particularly horticulture. At some sites, especially those in upland regions, aquatic vegetation covered much of the lake surface. Additional material was obtained from mangrove swamps located throughout Micronesia (Yap, Chuuk, and Pohnpei in the Federated States of Micronesia, and Guam), a region where precipitation is strongly influenced by the Intertropical Convergence Zone (ITCZ). All swamps were located at sea level and submerged at high tide. Four or five surface sediment samples were collected from each swamp along a transect from the inland edge of the swamp to the coast.

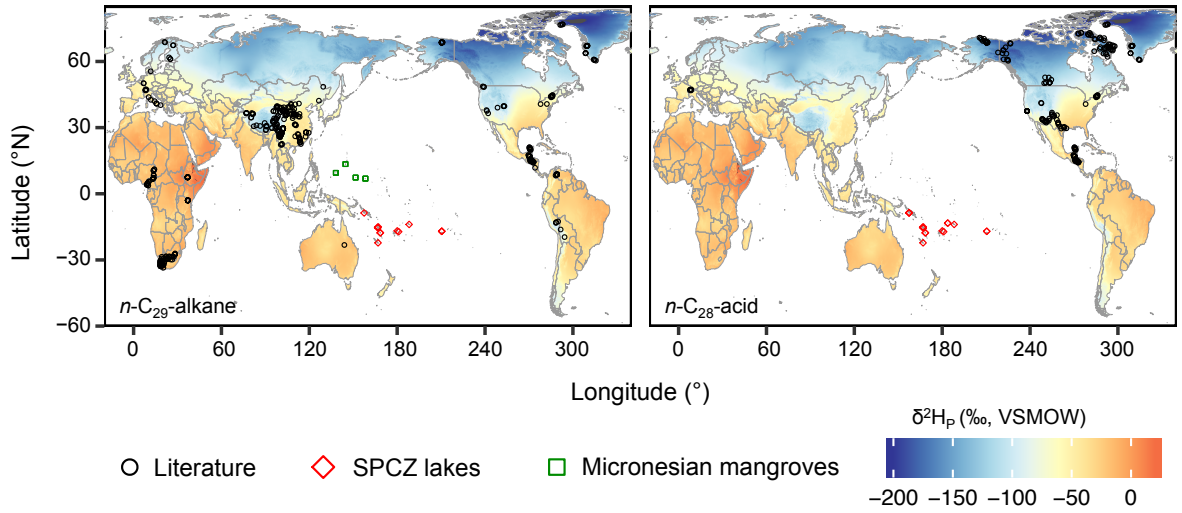

Figure 1 Map of the global distribution of leaf wax core-top samples from surface sediments and soils. The left panel shows the locations for *n*-C_{29}-alkane data (581 sites), while the right panel shows the locations for *n*-C_{28}-acid data (242 sites). Locations of samples in literature compilation are shown as black circles. Locations of new samples from this study are shown as red diamonds (lakes in the SPCZ region) and green squares (Micronesian mangrove swamps). Background shading represents mean annual δ^2H values of precipitation, as determined by the Online Isotopes in Precipitation Calculator (OIPC) (Bowen and Ravenaugh, 2003; IAEA/WMO, 2015; Bowen, 2020). OIPC does not produce spatial data sets over marine areas, therefore this shading is limited to continents.

Maloney et al. (2019) described the collection of most lake samples from the SPCZ region used for the present study. New samples include those from Lake Dranoniveilomo, which was cored in 2010 with a Universal Percussion Corer (Aquatic Research, Hope ID, USA) fitted with a 6.6 cm diameter polycarbonate core tube. Cores from lakes Vesalea and Nopovois were

collected in 2017 with a percussion corer (UWITEC, Mondsee, Austria) equipped with a 6.3 cm diameter polycarbonate tube. Unconsolidated sediment from the upper portion of these cores was subsampled at 1 cm intervals in the field and stored frozen in Whirl-Pak plastic bags (Nasco, Fort Atkinson, WI, USA). Farther north, mangrove swamp samples from the ITCZ region were collected in 2012 using a hand trowel to collect the upper 1 cm of mangrove peat and stored frozen in Whirl-Pak bags.

2.2 Leaf wax extraction and purification

Lipid extraction, saponification, and column chromatography for all lake surface sediments except Dranoniveilomo, Vesalea, and Nopovois were previously described by Maloney et al. (2019). Surface sediment from Dranoniveilomo was processed following the same protocol described in Maloney et al. (2019). Lipid extraction, saponification, and column chromatography from Vesalea was described by Krentscher et al. (2019), and was identical for the sample from Nopovois. Lipids from mangrove surface sediment was extracted and divided into compound classes using Si gel column chromatography as in Maloney et al. (2019).

For mangrove swamp samples, the *n*-alkanes were purified from the hexane fraction from Si gel columns by eluting 8 mL of 100% hexane over 0.5 g of of $AgNO_3$-impregnated Si gel (10% by weight). For lake samples, the hexane fraction from Si gel columns of neutral fractions was urea adducted to isolate unbranched compounds. Fatty acids from lake sediments were methylated with 5% HCl in methanol for 12 hours at 70 °C, and saturated fatty acid methyl esters (FAMEs) were isolated by eluting in 8 mL of 4:1 Hex/DCM over 0.5 g of $AgNO_3$-impregnated Si gel (10% by weight). Acid fractions were not analyzed from mangrove swamp samples. Purity and concentrations of *n*-alkanes from mangrove swamp samples was assessed by

gas chromatography – flame ionization detection (GC-FID) at the University of Washington in Seattle using the sample GC program and instrumentation described in Ladd and Sachs (2017). For swamp samples, *n*-alkane and *n*-acid homologues were quantified by GC-FID at Eawag in Kastanienbaum using the same GC program and instrumentation described in Ladd et al. (2018).

2.3 Leaf wax δ^2H measurements

Samples were dissolved in hexane at a concentration suitable for hydrogen isotope analyses of *n*-C_{29}-alkane or *n*-C_{28}-acid when those compounds were sufficiently abundant for analysis by gas chromatography – isotope ratio mass spectrometry (GC-IRMS). δ^2H values of other baseline-resolved homologues with peak areas greater than 15 Vs are also reported. For mangrove swamp samples, GC-IRMS analyses were conducted at the University of Washington in Seattle, using the same GC program and isotopic referencing described in Ladd and Sachs (2017). Lake sediment samples were measured at Eawag, in Kastanienbaum, Switzerland using the same GC program and isotopic referencing described in Ladd et al. (2018). An external quality control standard of *n*-C_{29}-alkane was measured three times throughout each sequence in Kastanienbaum and had an average value of -137 ± 4‰ (n = 42). The hydrogen added through methylation was determined by methylating phthalic acid of known isotopic composition (Shimmelmann, Indiana University) and measured δ^2H values of FAMEs were corrected by isotopic mass balance.

2.4 Estimates of mean annual precipitation δ^2H values

Annual mean estimates of precipitation δ^2H values were extracted from a variety of model products using the latitude, longitude, and elevation of collected samples. Model products

included the high resolution global grid from the Online Isotopes in Precipitation Calculator (OIPC) version 3.2 (Bowen and Ravenaugh, 2003; IAEA/WMO, 2015; Bowen, 2020), as well as isotope-enabled climate model contributions to the second Stable Water Isotope Intercomparison Group (SWING2) from the CAM, ECHAM, GISS ModelE, HadAM, isoGSM, LMDZ, and MIROC models (Sturm et al., 2010). For OIPC estimated values, values for each location were obtained by manually entering in the coordinates to the web interface ("OIPC mean annual d^2H"), and also by extracting the values from the available high-resolution spatial gridded data set using a bilinear smooth function to accommodate the proximity of a given location to neighboring pixels and the d^2H values from those pixels ("OIPC extracted mean annual d^2H"). An additional multi-model mean annual precipitation δ^2H value was also calculated by averaging predicted values for all climate model products that employed spectral nudging (Yoshimura et al., 2008), which includes the ECHAM, GISS (nudged), isoGSM, and LMDZ products.

2.5 Pollen counts

Core samples for palynomorph analyses (including pollen and spores) were taken from within the upper portion of the sediment core to determine modern baseline vegetation differences among lakes. Each 1 cm^3 sample was processed using standard procedures (10% HCl, hot 10% KOH, and acetolysis) (Moore et al. 1991). Samples were spiked with exotic *Lycopodium clavatum* L. tablets to allow the palynomorph and charcoal concentrations to be calculated. Counts continued until reaching a sum of at least 100 terrestrial palynomorphs. Reference palynomorphs held in the Australasian Pollen and Spore Atlas (apsa.anu.edu.au/) assisted with identification. The vegetation types (primary, secondary, dryland herbs, wetland

herbs, etc.) were determined from a regional synthesis of Pacific Island plant ecology (e.g. Mueller-Dombois and Fosberg 1998).

3 Results

3.1 Leaf wax δ^2H values in the tropical Pacific

Overall, δ^2H_{Wax} values from surface sediments in the tropical Pacific were not correlated with mean annual δ^2H_P values as calculated by the OIPC, nor with mean annual precipitation as estimated by the Global Precipitation Climatology Project (GPCP) (Figure 2; Table 2). The only lipids with significant correlations with δ^2H_P values were dinosterol (data from Maloney et al., 2019), *n*-C_{16}-acid, and *n*-C_{18}-acid, and the only significant correlations with mean annual precipitation were for dinosterol, *n*-C_{18}-acid, *n*-C_{17}-alkane, and *n*-C_{33}-alkane. In almost all cases,

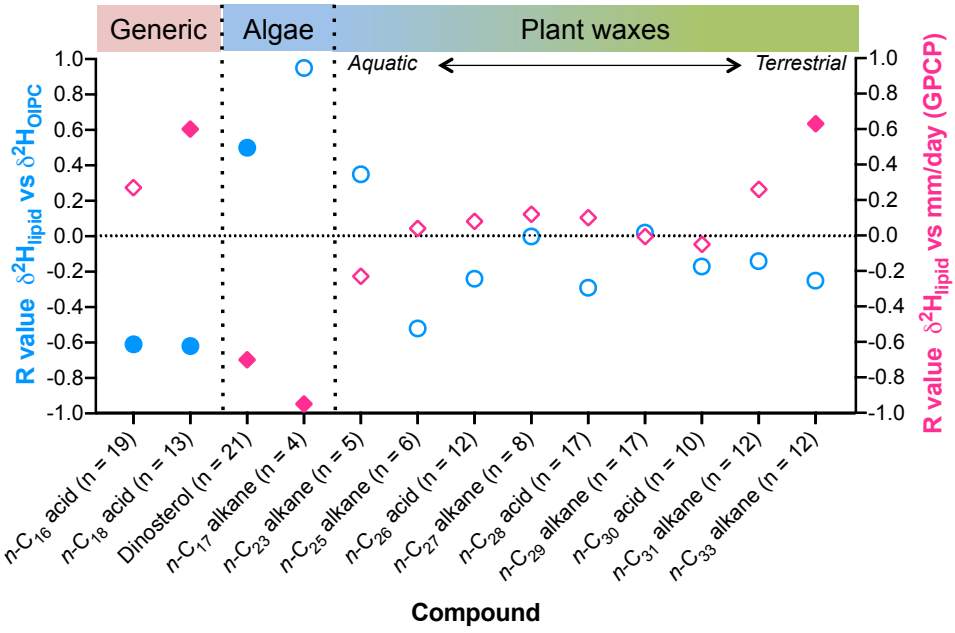

Figure 2: R values of linear regressions of δ^2H values of all analyzed compounds relative to tropical Pacific δ^2H_P values (blue circles) and relative to mean annual precipitation (pink diamonds). Filled symbols represent correlations that were significant at the 95% confidence level. Mean annual precipitation is from the Global Precipitation Climatology Project (GPCP) and δ^2H_P values are from the OIPC. Compounds are grouped by source (algal, general, or plant waxes, with increasingly likely terrestrial plant sources associated with longer chain lengths). Dinosterol δ^2H data is from Maloney et al. (2019), all other lipid δ^2H data from this study. Individual measurements are included in Data Set S1.

247 R values were negative for the relationship between δ^2H_{Wax} values and δ^2H_P values, and positive
248 for the relationship between δ^2H_{Wax} values and mean annual precipitation. A notable exception
249 was *n*-C_{17}-alkane, which, similarly to dinosterol, had δ^2H values that are negatively correlated
250 with mean annual precipitation (R = -0.95; p = 0.049) and positively correlated with δ^2H_P values
251 (R = 0.95; p = 0.051) (Figure 2). However, *n*-C_{17}-alkane was only present in high enough
252 concentrations for its δ^2H values to be measured in 4 samples, making the significance of these
253 correlations questionable.
254
255 3.2 Tropical Pacific δ^2H values in the global context
256 Tropical Pacific δ^2H values of *n*-C_{29}-alkanes and *n*-C_{28}-acids (the most commonly
257 measured leaf waxes in the literature) were in the range expected based on the global relationship
258 between δ^2H_{Wax} and δ^2H_P values (Figure 3). Tropical Pacific *n*-C_{29}-alkane δ^2H values ranged
259 from −177 to −139‰, while those of *n*-C_{28}-acid ranged from −175 to −119‰ (Table 1; Figure
260 3). At most tropical Pacific locations, residuals from the global linear regression line were within
261 ± 20‰, but were larger than this at 5 sites for *n*-C_{29}-alkane and at 6 sites for *n*-C_{28}-acid (Figure
262 3). Adding our new measurements to an updated global calibration curve between δ^2H_{Wax} and
263 δ^2H_P values (compilations from Liu and An, 2019 and McFarlin et al., 2019, as well as data sets
264 from Nelson, 2013; Bakkeland et al., 2018; Feng et al., 2019; Freimuth et al., 2019; Li et al.,
265 2019; Wu et al., 2019; Freimuth et al., 2020; Lu et al., 2020) has minimal impact on the slope, y-
266 intercept, or correlation coefficients for the global linear regression (Table 2).

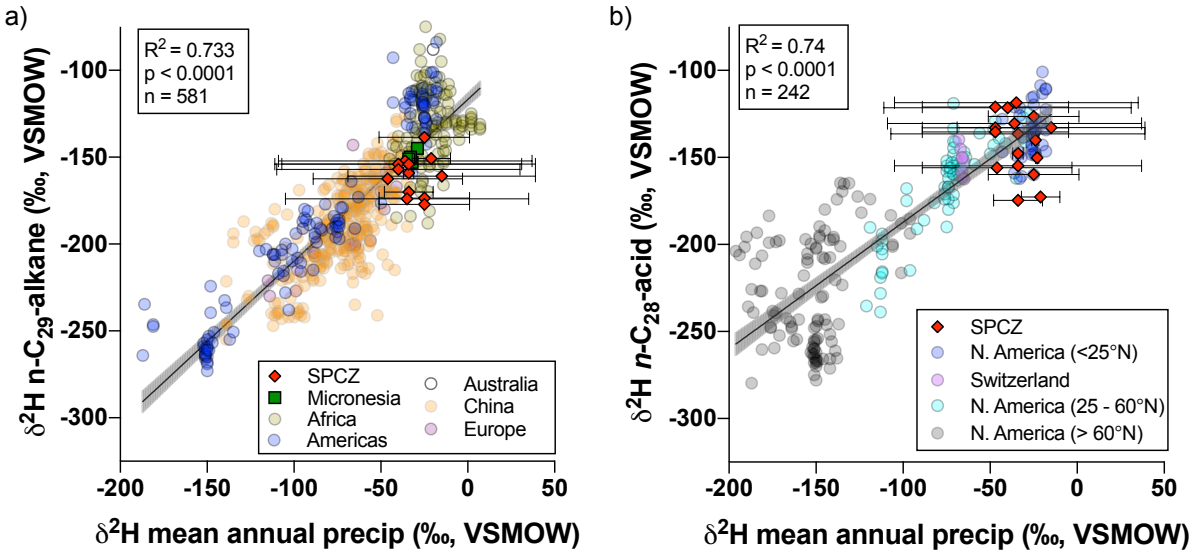

Figure 3 δ^2H values of (a) *n*-C_{29}-alkane and (b) *n*-C_{28}-acid from lacustrine surface sediments and surface soils plotted relative to δ^2H values of mean annual precipitation, as determined by the Online Isotopes in Precipitation Calculator (OIPC) (Bowen and Ravenaugh, 2003; IAEA/WMO, 2015; Bowen, 2020). Red diamonds are lakes from the SPCZ region (this study), and are plotted with error bars. Green squares are from mangrove swamps in Micronesia (this study) and are also plotted with error bars. In both cases, error bars on the x-axis represent 95% confidence intervals of OIPC values. Error bars on the y-axis represent 1 standard deviation of measurements from replicate sediment core-top samples from the same lake and are typically smaller than the marker size. Circles are global values compiled from the literature, and are color coded by region. For clarity, x-axis error bars on individual symbols are not shown for these previously published data points, and average 5.2‰ for sites outside the tropical Pacific. Shading around linear regression represents 95% confidence intervals. Regression statistics with and without the new Pacific data are reported in Table 2.

In addition to the OIPC, several water-isotope-enabled GCMs also provide estimates of mean annual δ^2H_P values. We extracted δ^2H_P values for all sites around the globe that have core-top δ^2H_{Wax} values from each climate model included in the Stable Water Isotope Intercomparison Group, Phase 2 (SWING 2) model comparison. For all models, global δ^2H_{Wax} was positively correlated with δ^2H_P for both *n*-C_{29}-alkane and *n*-C_{28}-acid (Figure 4). For *n*-C_{29}-alkane, global δ^2H_{Wax} values were most highly correlated with δ^2H_P values obtained manually from the OIPC (R = 0.87) and the lowest correlation was with δ^2H_P values from HadAM (R = 0.60) (Figure 4).

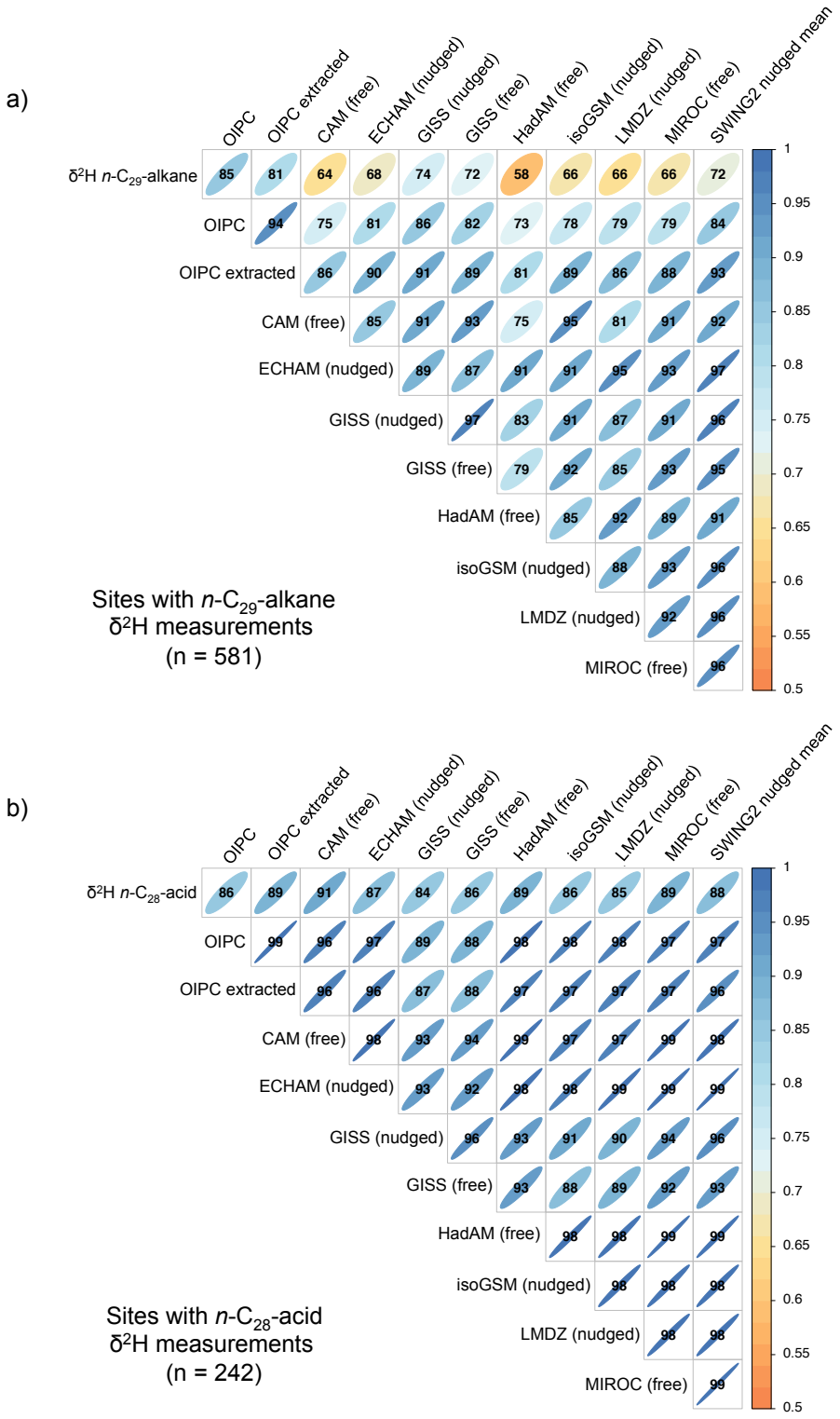

Figure 4 Correlation plots of δ^2H values from the global compilation of lacustrine surface sediments and surface soils relative to the δ^2H values of mean annual precipitation from various models (described in section 2.4). Panel a shows correlations for sites at which there are *n*-C_{29}-alkane δ^2H data, while panel b shows correlations for the sites at which there are *n*-C_{28}-acid δ^2H data. Numbers, colors, and the widths of the ellipses correspond to correlation coefficients (R values). Because the sites from which data for each compound is available from differ, the relationships for the cross-correlations among models is not consistent between the two analyses.

For *n*-C_{28}-acid, global δ^2H_{Wax} values were most highly correlated with δ^2H_P values extracted from the CAM model (R = 0.91), and the lowest correlation was with δ^2H_P values from the nudged GISS simulation (R = 0.84) (Figure 4). The correlation with δ^2H_P values obtained manually from the OIPC was on the lower end of this range (R = 0.86) (Figure 4). Overall, global δ^2H_P values were better correlated among model outputs for sites with core-top δ^2H_{Wax} values from *n*-C_{28}-acid (range of R values: 0.87 – 0.99) than for sites with core-top δ^2H_{Wax} values from *n*-C_{29}-alkane (range of R values: 0.74 – 0.97) (Figure 4).

3.3 Pollen and spore spectra

Palynomorphs from most sites was indicative of human disturbance to the catchment vegetation, as the dominant pollen types at most sites were secondary forest taxa (Figure 5; Table 3). In sites where secondary forest vegetation was not the most abundant type, ferns spores contributed more to the palynomorph sum than any other group of plants, except at Lake Hut, where primary forest taxa were most abundant (Figure 5; Table 3). Although more than 50% of the surface water at three lakes (Onetahi Pond, Lake Tagamucia, and Veselea Pond) was covered by wetland plants, wetland herbs and aquatic plants never contributed more than 23% of the observed pollen. Pollen data are only available for three of the five sites where the *n*-C_{29}-alkane residuals from the global δ^2H_{Wax} vs. δ^2H_P relationship was less than −20‰ (Figure 5). In two of these cases (Tagamaucia and White Lake), fern spores were recorded in high proportions (59% and 39%, respectively) (Figure 5; Table 3). However, at the third site with a high *n*-C_{29}-alkane residual (Lake Hut), fern spore concentrations were quite low and palynomorphs from primary forest taxa were the most abundant (Figure 5; Table 3). Three sites had *n*-C_{28}-acid residuals from the global δ^2H_{Wax} vs. δ^2H_P relationship that were less than −20‰, of which two have available

316 pollen data (Tagamaucia and Dranoniveilomo). Each of these had a high abundance of ferns and
317 wetland plants (80% and 37%, respectively) (Figure 5, Table 3). Three sites had *n*-C_{28}-acid
318 residuals from the global δ^2H_{Wax} vs. δ^2H_P relations that were greater than 20‰ (Figure 5). One of
319 these, White Lake, had relatively high contributions from ferns. The second, Harai Lake #1, does
320 not have recent pollen data (the most recent pollen sample available is from 11 – 12 cm), but
321 historically had greater contributions from ferns (Table 3). The third, Nopovois, is dominated by
322 secondary forest vegetation (54%) and does not have palynological features that clearly
323 distinguish it from sites where the *n*-C_{28}-acid δ^2H adhere more closely to the global relationship
324 (Figure 5; Table 3). Additionally, some sites with high contributions from ferns and wetland
325 plants – Harai Lake #3, Lanoto'o, and Lake Otas – have δ^2H_{Wax} values that fall close to the
326 global relationship (Figure 5).

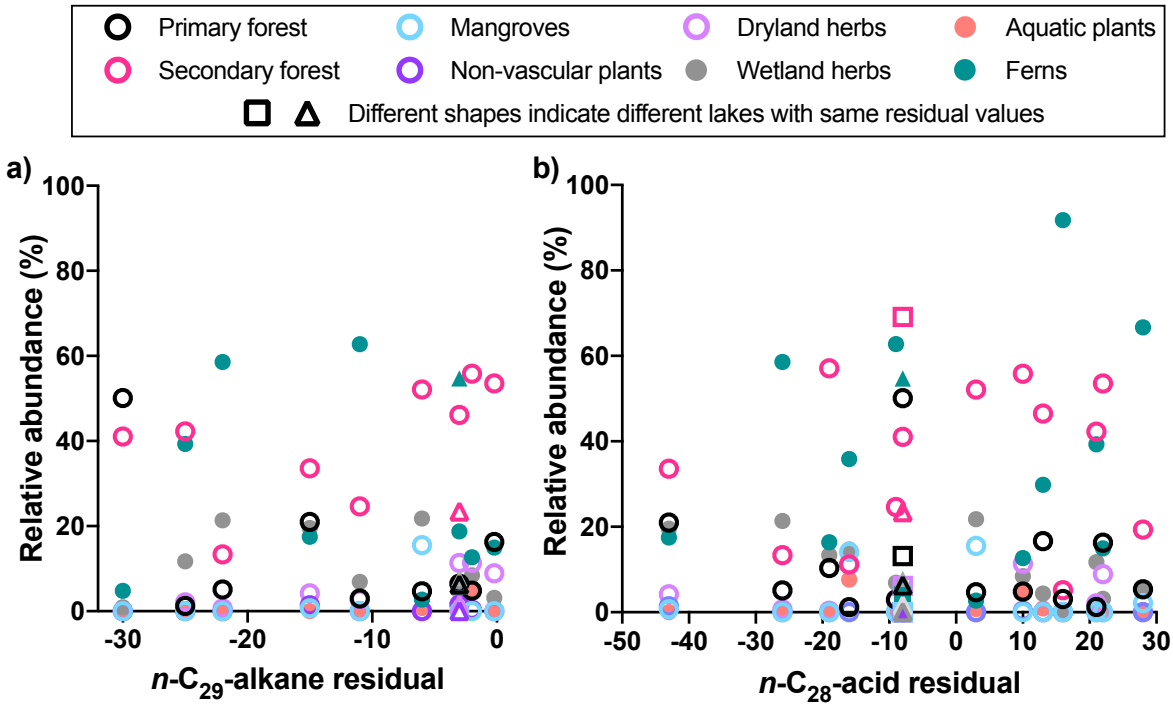

327
328 **Figure 5** Pollen distributions from surface or near surface sediments in tropical Pacific lake samples plotted relative
329 to residuals from the global $\delta^2H_{Wax} - \delta^2H_P$ calibration line for (a) *n*-C_{29}-alkane and (b) *n*-C_{28}-acid. Square and
330 triangle symbols are used to distinguish among multiple sites with the same residual values.
331
332

4 Discussion

Although the relationship between δ^2H_{Wax} values and δ^2H_P values lacks any clear correlation for the tropical Pacific sites in isolation, the values fall within the global scatter around the linear regression determined from a compilation of literature values from surface sediments in lakes and soils (Figure 3; Table 1). The positive linear relationship between δ^2H_{Wax} and δ^2H_P values remains robust, with R^2 values of 0.73 for *n*-C_{29}-alkane (n = 581) and 0.74 for *n*-C_{28}-acid (n = 242) (Figure 3; Table 2). However, considerable scatter around the regression line exists both globally and within the tropical Pacific. These large residuals are due to both uncertainty in the y-axis (variable $^2H/^1H$ fractionation between leaf waxes and water among plant types and environments, discussed in section 4.1) and in the x-axis (mean annual δ^2H_P values and the water source used by plants, discussed in section 4.2). These uncertainties should be kept in mind when interpreting down-core δ^2H_{Wax} records, and where possible, should be augmented by considering pollen distributions and δ^2H values of algal biomarkers.

4.1 Variable hydrogen isotope fractionation during synthesis of leaf waxes

Although global δ^2H_{Wax} values are generally well correlated with δ^2H_P values of mean annual precipitation (Figures 3, 4), several well-established factors are known to contribute to variability in the net $^2H/^1H$ fractionation between plant waxes and precipitation (α_{Wax}) (Sachse et al., 2012). Variations in α_{Wax} occur among plant functional types (Liu et al., 2006), between leaves and different plant organs (Gamarra and Kahmen, 2015), and with relative humidity (Tipple et al., 2015). Additionally, biosynthetic fractionation between leaf water and waxes can vary seasonally (Newberry et al., 2015), with environmental stresses (Ladd and Sachs, 2015), and with changes in plant metabolism (Cormier et al., 2018). Large differences in α_{Wax} can also exist among different species of plants growing at the same site (Feakins and Sessions, 2010;

Sachse et al., 2012; Eley et al., 2014; He et al., 2020). We examine three groupings of plants in particular whose contributions may significantly impact community δ^2H_{Wax} values: mangroves, aquatic plants, and ferns.

4.1.1 Mangroves

Mangroves are woody plants that can grow in brackish to hypersaline water, and they are common coastal plants in the tropics and subtropics, with significant contributions of organic matter to coastal sediments (Alongi, 2014). Because mangroves discriminate more against ^2H as salinity increases (Ladd and Sachs, 2012; He et al., 2017; Ladd and Sachs, 2017), their leaf waxes are expected to be ^2H-depleted relative to nearby freshwater plants. This relationship has recently been observed in the Florida Everglades, where mangroves produce leaf waxes that have δ^2H_{Wax} values that are ~ 50‰ lighter than nearby freshwater trees, despite the fact that δ^2H_P values are essentially constant for both groups (He et al., in press). Significant contributions of leaf waxes from mangroves, which may be especially prevalent in coastal areas in the tropical Pacific, could also result in sedimentary δ^2H_{Wax} values that fall below the global calibration line.

Several of the lakes in our calibration set were located in coastal areas, but only one, Dranoniveilomo, had brackish water and mangroves growing directly in its periphery. In this lake *n*-C_{28}-acid is significantly depleted relative to the global calibration, but *n*-C_{29}-alkane is not (Table 1). Although mangroves are present around the coastline of Dranoniveilomo, barely any mangrove pollen was found in the sediment, which may reflect different transport mechanisms and catchment areas for leaf waxes and pollen. Two coastal lakes in Vanuatu (Otas and Waérowa East) have the highest amounts of mangrove pollen observed of all examined surface sediments (~15%; Figure 5; Table 3). In Lake Otas δ^2H_{Wax} values are close to the values predicted by the

global relationship (Table 1). In Lake Waérowa East they are slightly higher than expected (Table 1), opposite to what would be caused by significant mangrove inputs of leaf waxes. These data suggest that waxes from mangroves do not have a large impact on sedimentary δ^2H_{Wax} values in the tropical Pacific lakes included in this study.

Likewise, Micronesian mangrove swamp surface sediments had δ^2H_{Wax} values that were consistent with the global linear regression (Table 1; Figure 3). Additionally, there was little spatial variability in δ^2H_{Wax} values throughout each individual mangrove swamp, with standard deviations for surface sediments within a single swamp typically in the range of 5‰ (Table 1). This homogeneity occurred even though samples were collected from sites with surface water salinity spanning a range of 0-31 at the time of collection. Surface water salinity was observed to be dynamic throughout these mangrove swamp surveys, varying temporally and spatially with tides and rain. Individual mangrove trees with large root networks would therefore have had access to water with a wide range of salinities and may have preferentially and opportunistically taken up relatively fresh water that was ultimately used in leaf wax synthesis. Preferential uptake of less saline water by mangroves has been observed previously (Santini et al., 2015; Reef et al., 2015), and could result in all mangroves throughout a swamp using water with a similar salinity and isotopic composition, consistent with the surface sediment δ^2H_{Wax} values observed in our transects from Micronesian mangrove swamps.

4.1.2 Aquatic plants

Some of the lakes included in the tropical Pacific survey were partially or completely covered by floating aquatic vegetation (Table 1). Since aquatic plants at diverse sites have been observed to have lower alkane δ^2H_{Wax} values than nearby terrestrial plants (Chikaraishi and

Naraoka, 2003; Gao et al., 2011; He et al., in press), differing relative contributions of leaf waxes from aquatic plants could also cause variability in sedimentary δ^2H_{Wax} values. There are a few reasons why aquatic plants might produce leaf waxes with relatively depleted δ^2H values. First, in the case where a lake is mostly covered by water lilies or similar aquatic vegetation, there is a physical barrier to evaporation of lake water, and it may therefore maintain a δ^2H signal that is more similar to that of precipitation, rather than becoming evaporatively enriched like the soil water used by terrestrial plants. Second, in the case of submerged aquatic plants, leaf water should be identical to lake water (Aichner et al., 2017), rather than being enriched in ^2H due to transpiration, as is the case for leaves exposed to air (Kahmen et al., 2013; Cernusak et al., 2016). It is also possible that aquatic plants may exhibit greater biosynthetic fractionation between leaf water and leaf lipids, but existing investigations of leaf wax δ^2H values in submerged aquatic plants suggest that is likely only at high salinity, with plants grown in freshwater displaying similar biosynthetic fractionation values to other plants (Aichner et al, 2017).

High contributions of leaf waxes from aquatic plants could, for example, explain why leaf waxes at Tagamaucia in Fiji were ^2H-depleted by more than 20‰ relative to the global calibration line (Table 1). However, this relationship was not consistent in all lakes with a significant presence of aquatic plants. For example, Lake Veselea in Vanuatu is completely covered by aquatic vegetation, yet δ^2H_{Wax} values from this system fell close to the global calibration line (Table 1). Additionally, pollen from wetland herbs and aquatic plants is not consistently associated with large or small residuals from the global calibration line (Figure 5). These patterns suggest that increased presence of aquatic plants does not unequivocally result in decreased δ^2H_{Wax} values. Minimal influence of aquatic plants on sedimentary δ^2H_{Wax} values may

426 be due to the fact that submerged plants are not at risk of desiccation and therefore have little
427 need for the moisture barrier provided by long-chain leaf waxes. They therefore tend to have low
428 concentrations of these compounds (Ficken et al., 2000; He et al., in press).
429
430 4.1.3 Ferns
431 There have been limited assessments of δ^2H_{Wax} values from ferns, but previous studies
432 show that ferns have similar $\alpha_{Wax\text{-}P}$ to many other plant taxa, including lycopods, gymnosperms,
433 eudicots, and magnoliids (Gao et al., 2014). We therefore had no expectation that sites with large
434 sedimentary contributions of leaf waxes from ferns would diverge from the global δ^2H_{Wax}-δ^2H_P
435 linear regression. However, some of the sites with the largest residuals relative to the global
436 regression line had palynomorph spectra that were characterized by large contributions of fern
437 spores. This was particularly true at Lakes Tagamaucia in Fiji and White Lake in Vanuatu, and to
438 a lesser extent in Fiji's Lake Dranoniveilomo (Table 1; Figure 5). However, high accumulation
439 of fern spores did not universally correspond to ^2H-depleted leaf waxes in our sample set, for
440 example at sites such as Lake Lanoto'o in Samoa and Harai Lakes #1 and #3 in the Solomon
441 Islands (Tables 1 and 3; Figure 5). Of these, fatty acid δ^2H values from the Harai Lakes were
442 much higher than the predicted values from the global regression fit, in direct contrast to the
443 Fijian lakes and White Lakes (Table 1; Figure 5). Additionally, Lake Hut in New Caledonia had
444 the largest *n*-C_{29} alkane residual for any site with pollen data, but did not have much fern pollen
445 (Figure 5). Overall, this suggests that relative contributions of leaf waxes from ferns do not have
446 predictable effects on sedimentary leaf wax δ^2H values. Nevertheless, a shift in δ^2H_{Wax} values
447 that coincides with a change in the relative abundance of fern spores in a down-core record may
448 be indicative of a change in organic matter sources rather than a change in δ^2H_P values.

449

450 4.2 Uncertainty in precipitation isotope values

451 Variability in $\alpha_{Wax\text{-}P}$ can be thought of as uncertainty in the y-axis in the relationship
452 between δ^2H_{Wax} and δ^2H_P (Figure 3). However, unlike in many proxy systems, the calibration
453 target on the x-axis is poorly constrained and likely accounts for a large portion of the residuals
454 observed in the linear regression between δ^2H_{Wax} and δ^2H_P values in the tropical Pacific. Notably,
455 the 95% confidence intervals on mean annual precipitation from the OIPC are more than twice as
456 large at some sites than the entire range of mean annual precipitation at our tropical Pacific sites
457 (76‰ relative to 32‰) (Figure 3). δ^2H_P values are not constant throughout the year, and water
458 from different seasons has different residence times in soil, meaning that the δ^2H values of water
459 used by plants is typically not equal to mean annual δ^2H_P values (Brinkmann et al., 2018).
460 Additionally, δ^2H_P values obtained from the OIPC represent climatological means, but δ^2H_P
461 values vary interannually and seasonally. The time period captured by a surface sediment sample
462 (typically a few years to two decades; see Maloney et al., 2019 for sediment accumulation rates
463 at most sites) may therefore differ considerably from the long-term mean. Finally, the robustness
464 of mean annual estimates provided by OIPC varies spatially among geographic settings and also
465 in response to the density of observations, which are not evenly distributed around the globe.
466 Limited δ^2H_P data from sites in the tropical Pacific mean that δ^2H_P values calculated using OIPC
467 have very large uncertainties (Table 1). The 95% confidence intervals in the δ^2H_P values from the
468 sites studied here are as large as 76‰, considerably larger than the overall range in δ^2H_P values
469 (~30‰) and the range in measured δ^2H_{Wax} values (~40‰ for *n*-C_{29}-alkane and ~55‰ for *n*-C_{28}-
470 acid) (Table 1; Figure 3). This uncertainty in the independent (x-axis) variable likely contributes
471 to the lack of a regional correlation between δ^2H_{Wax} and δ^2H_P values (Figure 3).

472 An alternative approach for estimating mean annual δ^2H_P values is to use water-isotope-
473 enabled GCMs (Sturm et al., 2010; Conroy et al., 2013; Steen-Larsen et al., 2017). These
474 estimates of δ^2H_P values have not typically been used in leaf wax δ^2H calibration studies, perhaps
475 because of the small uncertainties associated with OIPC estimates in other regions. Because
476 some of the western Pacific δ^2H_P values derived from OIPC had such large uncertainties, we
477 assessed whether scatter in the global relationship between δ^2H_{Wax} and δ^2H_P could be reduced by
478 using isotope-enabled GCMs to estimate δ^2H_P values. Specifically, we compared δ^2H_{Wax} values
479 to δ^2H_P values generated from each of the models included in the SWING2 intermodel
480 comparison study (Figure 4). For *n*-C_{29}-alkane, the δ^2H_P values derived from the OIPC were best
481 correlated with δ^2H_{Wax} values (Figure 4). For *n*-C_{28}-acid, the best correlation was not with values
482 from the OIPC, but the difference in correlation coefficients among different sources of δ^2H_P
483 estimates was overall much smaller than for *n*-C_{29}-alkane (Figure 4).

484 We also compared δ^2H_P values from each model output to values determined by the OIPC
485 for all sites that have core-top δ^2H_{Wax} data (Figure 4). Estimated δ^2H_P values were better
486 correlated with each other among sites from which core-top fatty acid data were available than
487 for sites with core-top *n*-alkane data (Figure 4), which likely reflects the different spatial
488 distribution of these data sets, and greater number of *n*-alkane measurements (581 vs. 242).
489 Besides our new data from the tropical Pacific and one previous study from central Europe (Ladd
490 et al., 2018), all of the sites with core-top fatty acid data are from North America (Figure 1). The
491 sites from which core-top *n*-alkane δ^2H values are available are more numerous, more globally
492 distributed, and include a high number of measurements from the Himalayas and Tibetan
493 Plateau. Here, steep elevation gradients may make precipitation isotopes vary on spatial scales
494 that are smaller than the resolution of most models, and where fluvial and aeolian processes may

transport waxes between regions with very different precipitation δ^2H values. Overall, this analysis does not suggest any structural limitations to using the OIPC to estimate δ^2H_P values for proxy calibration. However, the limited δ^2H_P measurements from the tropical Pacific and resulting large uncertainties in modern estimates from the OIPC or isotope-enabled GCMs remains a considerable challenge for assessing the fidelity of δ^2H_P values as a proxy for precipitation isotope values in this region.

In particular, the orographic effects of mountainous islands may not be adequately captured by either the OIPC or isotope-enabled GCMs, causing particular challenges determining the appropriate calibration target from water isotope proxies. For example, the highest peaks on the island of Espiritu Santo in Vanuatu are nearly 2000 m above sea level. With prevailing winds from the east, the west coast sits in the rain shadow of the mountains and is significantly drier than the eastern part of the island (Terry, 2011). However, the only long-term weather station for the island is located at Pekoa airport outside of Luganville in the southeast corner of the island, and there are no GNIP stations, meaning that minimal local data is available to inform precipitation isotope models. Although the leeward western sites would be expected to have lighter δ^2H_P values than the eastern sites that receive rain from more marine air masses, the OIPC predicts equivalent δ^2H_P values for lakes on opposite coasts of Espiritu Santo. Likewise, predicted δ^2H_P values from water-isotope-enabled GCMs for lakes on each coast are within a few ‰ of each other.

4.3 Different controls on δ^2H values of leaf waxes and lipids derived from other sources

In addition to the longer chain *n*-alkane and *n*-alkanoic acids that are primarily derived from higher plant waxes, we also measured δ^2H values from several compounds of mixed or

primarily algal sources. These compounds are typically found in sedimentary records along with leaf waxes, and the different controls on their δ^2H values offer the opportunity to more completely resolve sources of down-core variability in δ^2H_{Wax} values. Here we discuss lipids from algal sources, and ubiquitous compounds produced by most organisms.

4.3.1 Algal lipids

In general, δ^2H values of algal biomarkers are better correlated with tropical Pacific δ^2H_P values and mean annual precipitation than are δ^2H_{Wax} values (Figure 2). This is particularly the case for dinosterol (Maloney et al., 2019), a 4-methyl-sterol that is primarily produced by dinoflagellates (Volkman, 2003). The δ^2H values of *n*-C_{17}-alkane, which is primarily derived from algae (Cranwell et al., 1987; Meyers, 2003), was also highly correlated with δ^2H_P values (consistent with results of Sachse et al., 2004) and inversely correlated with mean annual precipitation (Figure 2). An inverse correlation between the amount of mean annual precipitation and δ^2H_P values (and therefore the δ^2H values of lipids that track δ^2H_P) values is expected in a low-latitude maritime region like the tropical Pacific where the amount effect plays a strong role in determining the isotopic composition of rain (Rozanski et al., 1993; Kurita et al., 2009).

One reason why δ^2H values from the algal biomarkers dinosterol and *n*-C_{17}-alkane are better correlated with δ^2H_P values than leaf waxes δ^2H values are might relate to the source water used by each type of organism. Leaf waxes from higher plants growing on land may reflect a temporal bias, as monthly OIPC δ^2H_P values can differ by up to 40 ‰ at the tropical Pacific sites with most seasonal variability in the Solomon Islands. Higher plants primarily produce leaf waxes soon after leaf flush (the setting of new leaves), meaning that there may be a seasonal bias in the water δ^2H signal that is transferred to their waxes (Tipple et al., 2013; Freimuth et al.,

2017). If algae are productive throughout the year, they may better integrate annual precipitation than the soil water accessed by trees, therefore resulting in algal lipids that more closely track mean annual δ^2H_P values.

Another reason why algal biomarkers track mean annual precipitation isotopes better than leaf waxes is that they come from a more limited range of potential sources. In addition to the range of plant sources for leaf waxes discussed in section 4.1, many of the mid-chain acetogenic compounds can be derived from a mix of terrestrial and aquatic sources (Bush and McInerney, 2013). Even the relatively long-chain *n*-C_{28}-acid can be partially derived from algal sources (Volkman, 1980; van Bree et al., 2018). This means that the leaf waxes may represent variable aquatic and terrestrial contributions, while the algal compounds are always aquatically sourced.

Finally, the spatial variability integrated by each type of compound could explain the different trends in their δ^2H_{Wax} values. Algal lipids are produced within the relatively confined space of the lake or pond overlaying the sediments in which they accumulate. Leaf waxes can be derived from plants growing adjacent to their depocenter, but also from further afield in the catchment, and the relative size of the catchment area can differ among water bodies. Additionally, a large portion of the leaf waxes accumulating in sediment are derived from leaf wax aerosols, which can be transported by wind and have δ^2H values that are not reflective of local vegetation (Conte et al., 2003; Gao et al., 2014; Nelson et al., 2017; Nelson et al., 2018). Distal leaf wax aerosols may have a greater impact on lake sediments on islands than on continents, since there is a relatively smaller contiguous land area to contribute regional and local waxes. On the other hand, the overall contribution of non-local leaf waxes may be significantly smaller on small islands where there is no adjacent landmass to provide regional-scale leaf waxes.

564

565 4.3.2 Generic fatty acids

566 In contrast to the algal specific biomarkers dinosterol and *n*-C_{17}-alkane, the δ^2H values of
567 *n*-C_{16} and *n*-C_{18} fatty acids were positively correlated with mean annual precipitation and
568 negatively correlated with δ^2H_P (Figure 2). These shorter chain fatty acids are synthesized by
569 most organisms, but are frequently attributed to algal sources in aquatic sediments (Huang et al.,
570 2004; Li et al. 2009). This is because short-chain fatty acids from terrestrial plant sources are
571 more susceptible to degradation during transport to sediments than those derived from algae (Ho
572 and Meyers, 1994; Canuel and Martens, 1996). Heterotrophic and chemoautotrophic microbes
573 produce short-chain fatty acids that can have δ^2H values that differ by several hundred ‰ from
574 those of photoautotrophs grown in similar water (Zhang et al., 2009; Heinzelmann et al., 2015).
575 However, other than in microbial mats (Osburn et al., 2011), sedimentary *n*-C_{16} and *n*-C_{18} fatty
576 acids typically have fractionation factors consistent with values from photoautotrophs in culture
577 (Li et al, 2009; Zhang et al., 2009; Heinzelmann et al., 2018). In our tropical Pacific data set,
578 fractionation factors between lake water and *n*-C_{16} and *n*-C_{18}-acids ($\alpha_{Lipid\text{-}Water} = (^2H/^1H)_{Lipid}/$
579 $(^2H/^1H)_{Water}$) ranged from 0.773 to 0.920. Although this range in $\alpha_{Lipid\text{-}Water}$ values is quite large,
580 it is consistent with the range observed in cultures of different types of algae (Zhang and Sachs,
581 2007; Zhang et al., 2009; Heinzelmann et al., 2015). The δ^2H values of the *n*-C_{16} and *n*-C_{18}-acids
582 in our data set could be influenced by variable contributions from non-photoautotrophs, but
583 could also encompass this range of values simply due to differing contributions from different
584 types of algae. In either case, it seems likely that the δ^2H values of these compounds are more
585 reflective of ecology than hydroclimate, and their negative correlation with δ^2H_P values may be a
586 coincidence in our sample set. Dinosterol and *n*-C_{17}-alkane are sourced from a smaller range of

organisms than the near ubiquitous *n*-C_{16} and *n*-C_{18}-acids (Cranwell et al., 1987; Meyers, 2003; Volkman, 2003), which could make their δ^2H values be more directly related to those of water.

4.4 Implications for paleoclimate reconstructions in the tropical Pacific

Although δ^2H_{Wax} values are strongly linearly correlated with δ^2H_P values on a global scale (Figure 3), the large residuals in this relationship indicate that caution should be applied before interpreting relatively small down-core changes in δ^2H_{Wax} values as hydroclimate changes. However, our data do not suggest that there are clear links between vegetation source (as indicated by palynological analyses) and δ^2H_{Wax}-δ^2H_P residuals from the global relationship. Rather, the largest challenge for interpreting sedimentary δ^2H_{Wax} values in the tropical Pacific are related to the uncertainties associated with modern estimates of precipitation δ^2H values in this region. Recent isotope modeling work has helped constrain the processes that control δ^2H_P values in this dynamically important region (Conroy et al., 2016; Konecky et al., 2019). Continued effort in this regard is necessary to robustly interpret proxy values of past precipitation isotopes, whether they are derived from sedimentary leaf waxes or from other archives such as speleothems.

Hydroclimate-driven interpretations of changes in sedimentary δ^2H_{Wax} values will be most robust if they can be supported by independent lines of proxy evidence, such as δ^2H values of more source specific biomarkers such as dinosterol (Smittenberg et al., 2011; Nelson and Sachs, 2016; Richey and Sachs, 2016; Maloney et al., 2019), changes in grain size distributions (Conroy et al., 2008), or changes in the elemental composition of inorganic sediments (Sear et al 2020; Higley et al., 2018). Continued refinement of a multi-proxy toolbox that includes

609 sedimentary δ^2H_{Wax} values offers the best path to confidently reconstructing past hydrologic
610 change in the tropical Pacific.

611 **5 Conclusions**

612 δ^2H_{Wax} values from surface sediments from 23 lakes and swamps on 15 islands throughout
613 the western tropical Pacific fall within the overall range of values expected based on a global
614 compilation surface sediment measurements ($R^2 = 0.73$, n = 581 for *n*-C_{29}-alkane; $R^2 = 0.74$, n =
615 242 for *n*-C_{28}-acid), and the residuals around the global linear regression between δ^2H_{Wax} and
616 δ^2H_P are similar in the tropical Pacific and global data sets. Nevertheless, within the tropical
617 Pacific there is no significant correlation between δ^2H_{Wax} and δ^2H_P values. The lack of correlation
618 regionally is at least partly due to the large uncertainties in δ^2H_P values derived from reanalysis
619 data and cannot be ascribed to different vegetation sources within and surrounding the lakes in
620 this study, as deduced from pollen assemblages.

621 To a first order on a global scale, δ^2H_{Wax} values clearly reflect δ^2H_P values and can be
622 interpreted in lake sediments from tropical Pacific islands in a manner similar to other locations
623 around the globe. The same limitations that affect δ^2H_{Wax} values in other locations apply to the
624 tropical Pacific. In particular, interpretations need to consider the possible effects of changing
625 source vegetation, growth conditions, and delivery of leaf waxes to sediments. Any hydroclimate
626 interpretations of δ^2H_{Wax} values need to be informed by the complex factors that control δ^2H_P
627 values in the tropical Pacific. When possible, δ^2H_{Wax} values should be paired with δ^2H values of
628 more source-specific compounds such as the dinoflagellate biomarker dinosterol, which can help
629 distinguish changes in water isotopes from changes in the various factors that affect α_{Wax} values.
630 As is the case for all paleoclimate proxies, interpretations of δ^2H_{Wax} values are most robust in a
631 multiproxy context.

Acknowledgments, Samples, and Data

This work was funded by a Swiss National Science Foundation grant to ND (Grant Nr. PP00P2_163782), a National Science Foundation grant to JPS (Grant No. 1502417), a NERC grant to DAS (NE/N00674/1), and an Australian Research Council grant to MP (DP0985593). Carsten Schubert hosted NL for laboratory work and provided access to the necessary instrumentation. Nichola Strandberg provided pollen data from the Lake Hut core-top. Christiane Krentscher helped with sample processing in addition to those thanked for lab work by Maloney et al. (2019). Many people helped with sample collection, as listed in Maloney et al. (2019) and Krentscher et al. (2019). All data associated with this manuscript is freely available in the ETH data repository (doi: 10.3929/ethz-b-000412154).

References

Aichner, B., Herzschuh, U., Wilkes, H., Vieth, A., Böhner, & J. (2010). δD values of n-alkanes in Tibetan lake sediments and aquatic macrophytes–A surface sediment study and application to a 16 ka record from Lake Koucha. *Organic Geochemistry*, *41*(8), 779-790. https://doi.org/10.1016/j.orggeochem.2010.05.010

Aichner, B., Hilt, S., Périllon, C., Gillefalk, M., & Sachse, D. (2017). Biosynthetic hydrogen isotopic fractionation factors during lipid synthesis in submerged aquatic macrophytes: Effect of groundwater discharge and salinity. *Organic Geochemistry*, *113*, 10-16. https://doi.org/10.1016/j.orggeochem.2017.07.021

Alongi D. M. (2014). Carbon cycling and storage in mangrove forests. *Annual Review of Marine Science*, *6*, 195-219. https://doi.org/10.1146/annurev-marine-010213-135020

Bai, Y., Fang, X., Gleixner, G., & Mügler, I. (2011). Effect of precipitation regime on dD valuesügler, I., 2011. Effect of precipitation regime on δD values of soil n-alkanes from elevation gradients – implications fort he study of paleoelevation. *Organic Geochemistry*, *42*(7), 838-845. https://doi.org/10.1016/j.orggeochem.2011.03.019

Bakkelund, A., Porter, T. J., Froese, D. G., & Feakins, S. J. (2018). Net fractionation of hydrogen isotopes in *n*-alkanoic acids from soils in the northern boreal forest. *Organic Geochemistry*, *125*, 1-13. https://doi.org/10.1016/j.orggeochem.2018.08.005

Bowen, G. J. (2020). The Online Isotopes in Precipitation Calculator, version 3.1. http://www.waterisotopes.org.

Bowen, G. J., & Ravenaugh, J. (2003). Interpolating the isotopic composition of modern meteoric precipitation. *Water Resources Research*, *39*(10), 1-13. https://doi.org/10.1029/2003WR002086

Bowen, G. J., Cai, Z., Fiorella, R. P., & Putman, A. L. (2019). Isotopes in the water cycle: regional- to global-scale patterns and applications. *Annual Review of Earth and Planetary Sciences*, *47*, 453-479. https://doi.org/10.1146/annurev-erath-053018-060220

Brinkmann, N., Seeger, S., Weiler, M., Buchmann, N., Eugster, W., & Kahmen, A. (2018). Employing stable isotopes to determine the residence times of soil water and the temporal origin of water taken up by *Fagus sylvatica* and *Picea abies* in a temperate forest. *New Phytologist*, *219*(4), 1300-1313. https://doi.org/10.1111/nph.15255

Brown, J. R., Moise, A. F., & Delage, F. P. (2011). Changes in the South Pacific Convergence Zone in IPCC AR4 future climate projections. *Climate Dynamics*, *39*, 1-19. https://doi.org/10.1007/s00382-011-1192-0

675 Bush, R. T., & Mcinerney, F. A. (2013). Leaf wax n-alkane distributions in and across modern
676 plants: implications for paleoecology and chemotaxonomy. *Geochimica et Cosmochimica*
677 *Acta*, *117*, 161-179. https://doi.org/10.1016/j.gca.2013.04.016
678 Calvo, E., Marshall, J. F., Pelejero, C., McCulloch, M. T., Gagan, M. K., & Lough, J. M. (2007).
679 Interdecadal climate variability in the Coral Sea since 1708 A.D. *Palaeogeography,*
680 *Palaeoclimatology, Palaeoecology*, *248*(1-2), 190-201.
681 https://doi.org/10.1016/j.palaeo.2006.12.003
682 Canuel E. A., & Martens C. S. (1996). Reactivity of recently deposited organic matter:
683 Degradation of lipid compounds near the sediment–water interface. *Geochimica et*
684 *Cosmochimica Acta*, *60*(10), 1793–1806. https://doi.org/10.1016/0016-7037(96)00045-2
685 Cernusak, L. A., Barbour, M. M., Arndt, S. K., Cheesman, A. W., English, N. B., Feild, T. S., et
686 al. (2016). Stable isotopes in leaf water of terrestrial plants. *Plant, Cell and Environment*,
687 *39*(5), 1087-1102. https://doi.org/10.1111/pce.12703
688 Chikaraishi Y., & Naraoka H. (2003). Compound-specific δD-δ^{13}C analyses of n-alkanes
689 extracted from terrestrial and aquatic plants. *Phytochemistry*, *63*(3), 361–371.
690 https://doi.org/10.1016/S0031-9422(02)00749-5
691 Conroy, J. L., Cobb, K. M., & Noone, D. (2013). Comparison of precipitation isotope variability
692 across the tropical Pacific in observations and SWING2 model simulations. *JGR*
693 *Atmospheres*, *118*(11), 5867-5829. https://doi.org/10.1002/jgrd.50412
694 Conroy, J. L., Noone, D., Cobb, K. M., Moerman, J. W., & Konecky, B. L. (2016). Paired stable
695 isotopologues in precipitation and vapor: A case study of the amount effect within western
696 tropical Pacific storms. *JGR Atmospheres*, *121*(7), 3290-3303.
697 https://doi.org/10.1002/2015JD023844
698 Conte, M. H., Weber, J. C., Carlson, P. J., & Flanagan, L. B. (2003). Molecular and carbon
699 isotopic composition of leaf wax in vegetation and aerosols in a northern prairie
700 ecosystem. *Oecologia*, *135*, 67-77. https://doi.org/10.1007/s00442-002-1157-4
701 Cormier, M. -A., Werner, R. A., Sauer, P. E., Grocke, D. R., Leuenberger, M. C., Wieloch, T., et
702 al. (2018). ^{2}H-fractionations during the biosynthesis of carbohydrates and lipids imprint a
703 metabolic signal on the δ^{2}H values of plant organic compounds. *New Phytologist*, *218*(2),
704 479-491. https://doi.org/10.1111/nph.15016
705 Cranwell, P. A., Eglinton, G., & Robinson, N. (1987). Lipid of aquatic organisms as potential
706 contributors to lacustrine sediments II. *Organic Geochemistry*, *11*(6), 513-527.
707 https://doi.org/10.1016/0146-6380(87)90007-6
708 Daniels, W. C., Russell, J. M., Giblin, A. E., Welker, J. M., Klein, E. S., & Huang, Y. (2017).
709 Hydrogen isotope fractionation in leaf waxes in the Alaskan Arctic tundra. *Geochimica et*
710 *Cosmochimica Acta*, *213*, 216-236. https://doi.org/10.1016/j.gca.2017.06.028
711 DeLong, K. L., Quinn, T. M., Taylor, F. W., Lin, K., & Shen, C. -C. (2012). Sea surface
712 temperature variability in the southwest tropical Pacific since 1649. *Nature Climate*
713 *Change*, *2*, 799-804. https://doi.org/10.1038/NCLIMATE1583
714 Douglas, P. M. J., Pagani, M., Brenner, M., Hodell, D. A., & Curtis, J. H. (2012). Aridity and
715 vegetation composition are important determinants of leaf-wax δD values in southeastern
716 Mexico and Central America. *Geochimica et Cosmochimica Acta*, *97*, 24-45.
717 https://doi.org/10.1016/j.gca.2012.09.005
718 Eley, Y., Dawson, L., Black, S., Andrews, J., & Pendentchouk, N. (2014). Understanding ^{2}H/^{1}H
719 systematics of leaf wax *n*-alkanes in coastal plants at Stiffkey saltmarsh, Norfolk, UK.
720 *Geochimica et Cosmochimica Acta, 128*, 13-28. https://doi.org/10.1016/j.gca.2013.11.045

Feakins, S. J., & Sessions, A. L. (2010). Controls on the D/H ratios of plant leaf waxes in an arid ecosystem. *Geochimica et Cosmochimica Acta*, *74*(7), 2128-2141. https://doi.org/10.1016/j.gca.2010.01.016

Feng, X., D'Andrea, W. J., Zhao, C., Xin, S., Zhang, C., & Liu, W. (2019). Evaluation of leaf wax δD and soil brGDGTs as tools for paleoaltimetry on the southeastern Tibetan Plateau. *Chemical Geology*, *523*, 95-106. https://doi.org/10.1016/j.chemgeo.2019.05.005

Ficken, K. J., Li, B., Swain, D. L., & Eglinton, G. (2000). An *n*-alkane proxy for the sedimentary input of submerged/floating freshwater aquatic macrophytes. *Organic Geochemistry, 31*(7-8), 745-749. https://doi.org/10.1016/S0146-6380(00)00081-4

Freimuth, E. J., Diefendorf, A. F., & Lowell, T. V. (2017). Hydrogen isotopes of *n*-alkanes and *n*-alkanoic acids as tracers of precipitation in a temperate forest and implications for paleorecords. *Geochimica et Cosmochimica Acta, 206*, 166-183. https://doi.org/10.1016/j.gca.2017.02.027

Freimuth, E. J., Diefendorf, A. F., Lowell, T. V., Bates, B. R., Schartman, A., Bird, B. W., et al. (2020). Contrasting sensitivity of lake sediment *n*-alkanoic acids and *n*-alkanes to basin-scale vegetation and regional-scale precipitation δ2H in the Adirondack Mountains, NY (USA). *Geochimica et Cosmochimica Acta*, *268*, 22-41. https://doi.org/10.1016/j.gca.2019.08.026

Freimuth, E. J., Diefendorf, A. F., Lowell, T. V., & Wiles, G. C. (2019). Sedimentary n-alkanes and n-alkanoic acids in a temperate bog are biased toward woody plants. *Organic Geochemistry*, *128*, 94-107 https://doi.org/10.1016/j.orggeochem.2019.01.006

Gamarra, B., & Kahmen, A. (2015). Concentrations and δ^2H values of cuticular *n*-alkanes vary significantly among plant organs, species and habitats in grasses from an alpine and a temperate European grassland. *Oecologia, 178*, 981-998. https://doi.org/10.1007/s00442-015-3278-6

Gao L., Edwards E. J., Zeng Y., & Huang Y. (2014). Major Evolutionary Trends in Hydrogen Isotope Fractionation of Vascular Plant Leaf Waxes. *PLoS ONE, 9*(11): e112610. https://doi.org/10.1371/journal.pone.0112610

Gao, L., Hou, J., Toney, J., MacDonald, D., & Huang, Y. (2011). Mathematical modeling of the aquatic macrophyte inputs of mid-chain *n*-alkyl lipids to lake sediments: implications for interpreting compound specific hydrogen isotopic records. *Geochimica et Cosmochimica Acta, 75*(13), 3781-3791. https://doi.org/10.1016/j.gca.2011.04.008

Garcin, Y., Schwab, V. F., Gleixner, G., Kahmen, A., Todou, G., Sene, O., et al. (2012). Hydrogen isotope ratios of lacustrine sedimentary n-alkanes as proxies of tropical African hydrology: insights from a calibration transect across Cameroon. *Geochimica et Cosmochimica Acta, 79*, 106-126. https://doi.org/10.1016/j.gca.2011.11.039

Gillespie, T. W., Keppel, G., Pau, S., Price, J. P., Jaffre, T., & O'Neill, K. (2013). Scaling species richness and endemism of tropical dry forests on oceanic islands. *Diversity and Distributions, 19*(8), 896-906. https://doi.org/10.1111/ddi.12036

Gosling, W. D., Sear, D. A., Hassall, J. D., Langdon, P. G., Bönnen, M. N. T., Driessen, T. D., & McMichael, C. N. H. (2020). Human occupation and ecosystem change on Upolu (Samoa) during the Holocene. *Journal of Biogeography, 47*(3), 600-614. https://doi.org/10.1111/jbi.13783

Hassall, J. D. (2017). Static or dynamic: Reconstructing past movement of the South Pacific Convergence Zone. University of Southampton.

He, D., Ladd, S. N., Sachs, J. P., & Jaffé, R. (2017). Inverse relationship between salinity and $^{2}H/^{1}H$ fractionation in leaf wax n-alkanes from Florida mangroves. *Organic Geochemistry, 110*, 1-12. https://doi.org/10.1016/j.orggeochem.2017.04.007

He, D., Ladd, S. N., Saunders, C. J., Mead, R. N., & Jaffé, R. (2019). Distribution of *n*-alkanes and their $\delta^{2}H$ and $\delta^{13}C$ values in typical plants along a terrestrial-coastal-oceanic gradient. *Geochimica et Cosmochimica Acta*, *281*, 31-52. https://doi.org/10.1016/j.gca.2020.05.003

Hendy, E. J., Gagan, M. K., Alibert, C. A., McCulloch, M. T., Lough, J. M., & Isdale, P. J. (2002). Abrupt decrease in tropical Pacific sea surface salinity at end of Little Ice Age. *Science, 295*(5559), 1511-1514. https://doi.org/10.1126/science.1067693

Heinzelmann, S. M., Villanueva, L., Lipsewers, Y. A., Sinke-Schoen, D., Sinninghe Damsté, J. S., Schouten, S., & van der Meer, M. T. J. (2018). Assessing the metabolism of sedimentary microbial communities using the hydrogen isotope composition of fatty acids. *Organic Geochemistry, 124*, 123-132. https://doi.org/10.1016/j.orggeochem.2018.07.011

Heinzelmann S. M., Villanueva L., Sinke-Schoen D., Sinninghe Damsté J. S., Schouten S., & van der Meer M. T. J. (2015). Impact of metabolism and growth phase on the hydrogen isotopic composition of microbial fatty acids. *Frontiers in Microbiology, 6*, 408. https://doi.org/10.3389/fmicb.2015.00408

Hermann, N., Boom, A., Carr, A. S., Chase, B. M., West, A. G., Zabel, M., Schefuss, E. (2017). Hydrogen isotope fractionation of leaf wax *n*-alkanes in southern African soils. *Organic Geochemistry, 109*, 1-13. https://doi.org/10.1016/j.orggeochem.2017.03.008

Higley, M. C., Conroy, J. L., & Schmitt, S. (2018). Last Millennium Meridional Shifts in Hydroclimate in the Central Tropical Pacific. *Paleoceanography and Paleoclimatology, 33*(4), 354-366. https://doi.org/10.1002/2017PA003233

Ho E. S., & Meyers, P. A. (1994). Variability of early diagenesis in lake sediments: Evidence from the sedimentary geolipid record in an isolated tarn. *Chemical Geology, 112*(3-4), 309–324. https://doi.org/10.1016/0009-2541(94)90031-0

Hope, G. S., & Pask, J. (1998). Tropical vegetational change in the late Pleistocene of New Caledonia. *Palaeogeography, Palaeoclimatology, Palaeoecology, 142*(1-2), 1-21. https://doi.org/10.1016/S0031-0182(97)00140-5

Hou, J., D'Andrea, W., & Huang, Y. (2008). Can sedimentary leaf waxes record D/H ratios of continental precipitation? Field, model and experimental assessments. *Geochimica et Cosmochimica Acta, 72*(14), 3503-3517. https://doi.org/10.1016/j.gca.2008.04.030

Huang, Y., Shuman, B., Wang, Y., & Webb III, T. (2004). Hydrogen isotope ratios of individual lipids in lake sediments as novel tracers of climatic and environmental change: a surface sediment test. *Journal of Paleolimnology, 31*, 363-375. https://doi.org/10.1023/B:JOPL.0000021855.80535.13

IAEA/WMO (2015). Global Network of Isotopes in Precipitation. The GNIP Database. Accessible at: https://nucleus.iaea.org/wiser.

Jaeschke, A., Rethemeyer, J., Lappe, M., Schouten, S., Boeckx, P., & Schefuss, E. (2018). Influence of land use of distribution of soil *n*-alkane δD and brGDGTs along an altitudinal transect in Ethiopia: Implications for (paleo)environmental studies. *Organic Geochemistry, 124*, 77-87. https://doi.org/10.1016/j.orggeochem.2018.06.006

Jia, G., Wei, K., Chen, F., & Peng, P. (2008). Soil *n*-alkane δD vs. altitude gradients along Moung Gongga, China. *Geochimica et Cosmochimica Acta, 72*(21), 5165-5174. https://doi.org/10.1016/j.gca.2008.08.004

Kahmen, A., Hoffmann, B., Schefuss, E., Arndt, S. K., Cernusak, L. A., West, J. B., & Sachse, D. (2013). Leaf water deuterium enrichment shapes leaf wax n-alkane δD values of angiosperm plants II: Observational evidence and global implications. *Geochimica et Cosmochimica Acta, 111*, 50–63. https://doi.org/10.1016/j.gca.2012.09.004

Konecky, B. L., Noone, D. C., & Cobb, K. M. (2019). The influence of competing hydroclimate processes on stable isotope ratios in tropical rainfall. Geophysical Research Letters 46(3), 1622-1633. https://doi.org/10.1029/2018GL080188

Konecky, B. L., Russell, J., & Bijaksana, S. (2016). Glacial aridity in central Indonesia coeval with intensified monsoon circulation. *Earth and Planetary Science Letters 437*, 15-24. https://doi.org/10.1016/j.epsl.2015.12.037

Krentscher, C., Dubois, N., Camperio, G., Prebble, M., Ladd, S.N., 2019. Palmitone as a potential species-specific biomarker for the crop plant taro (*Colocasia esculenta Schott*) on remote Pacific islands. *Organic Geochemistry, 132*, 1-10. https://doi.org/10.1016/j.orggeochem.2019.03.006

Kurita, N., Ichiyanagi, K., Matsumoto, J., Yamanaka, M. D., & Ohata, T. (2009). The relationship between the isotopic content of precipitation and the precipitation amount in tropical regions. *Journal of Geochemical Exploration, 102*(3), 113-122. https://doi.org/10.1016/j.gexplo.2009.03.002

Ladd S. N., & Sachs J. P. (2012). Inverse relationship between salinity and n-alkane δD values in the mangrove *Avicennia marina*. *Organic Geochemistry, 48*, 25–36. https://doi.org/10.1016/j.orggeochem.2012.04.009

Ladd, S. N., & Sachs, J. P. (2015). Influence of salinity on hydrogen isotope fractionation in *Rhizophora* mangroves from Micronesia. *Geochimica et Cosmochimica Acta, 168*, 206–221. https://doi.org/10.1016/j.gca.2015.07.004

Ladd, S. N., & Sachs, J. P. (2017). $^{2}H/^{1}H$ fractionation in lipids of the mangrove *Bruguiera gymnorhiza* increases with salinity in marine lakes of Palau. *Geochimica et Cosmochimica Acta, 204*, 300-312. https://doi.org/10.1016/j.gca.2017.01.046

Ladd, S. N., Nelson, D. B., Schubert, C. J., & Dubois, N. (2018). Lipid compound classes display diverging hydrogen isotope responses in lakes along a nutrient gradient. *Geochimica et Cosmochimica Acta, 237*, 103-119. https://doi.org/10.1016/j.gca.2018.06.005

Leider, A., Hinrichs, K. -U., Schefuss, E., & Versteegh, G. J. M. (2013). Distribution and stable isotopes of plant wax derived n-alkanes in lacustrine, fluvial and marine surface sediments along an Eastern Italian transect and their potential to reconstruct the hydrological cycle. *Geochimica et Cosmochimica Acta, 117*, 16-32. https://doi.org/10.1016/j.gca.2013.04.018

Li C., Sessions A. L., Kinnaman F. S., & Valentine D. L. (2009). Hydrogen-isotopic variability in lipids from Santa Barbara Basin sediments. *Geochimica et Cosmochimica Acta, 73*, 4803-4823. https://doi.org/10.1016/j.gca.2009.05.056

Li, Y., Yang, S., Luo, P., & Xiong, S. (2019). Aridity-controlled hydrogen isotope fractionation between soil *n*-alkanes and precipitation in China. *Organic Geochemistry, 133*, 53-64. https://doi.org/10.1016/j.orggeochem.2019.04.009

Linsley, B. K., Kaplan, A., Gouriou, Y., Salinger, J., DeMenocal, P., Wellington, G. M., & Howe, S. S. (2006). Tracking the extent of the South Pacific Convergence Zone since the early 1600s. *Geochemistry, Geophysics, and Geosystems, 7*, 1-15. https://doi.org/10.1029/2005GC001115

Linsley, B. K., Wellington, G. M., Schrag, D. P., Ren, L., Salinger, M. J., & Tudhope, A. W. (2004). Geochemical evidence from corals for changes in the amplitude and spatial pattern of South Pacific interdecadal climate variability over the last 300 years. *Climate Dynamics, 22*, 1-11. https://doi.org/10.1007/s00382-003-0364-y

Liu, J., & An, Z. (2019). Variations in hydrogen isotope fractionation in higher plants and sediments across different latitudes: Implications for paleohydrological reconstruction. *Science of the Total Environment, 650*(1), 470-478. https://doi.org/10.1016/j.scitotenv.2018.09.047

Liu, W. G., Yang, H., & Li, L. (2006). Hydrogen isotopic composition of n-alkanes from terrestrial plants correlate with their ecological life form. *Oecologia, 150*, 330-338. https://doi.org/ 10.1007/s00442-006-0494-0

Lu, J., Zang, J., Meyers, P., Huang, X., Qiu, P., Yu, X., et al. (2020). Surface soil *n*-alkane molecular and δD distributions along a precipitation transect in northeastern China. *Organic Geochemicstry 144*, 104015. https://doi.org/10.1016/j.orggeochem.2020.104015

Maloney, A. E., Nelson, D. B., Richey, J. N., Prebble, M., Sear, D. A., Hassell, J. D., et al. (2019). Reconstructing precipitation in the tropical South Pacific from dinosterol $^{2}H/^{1}H$ ratios in lake sediment. *Geochimica et Cosmochimica Acta, 245*, 190-206. https://doi.org/10.1016/j.gca.2018.10.028

Maupin, C. R., Partin, J. W., Shen, C. -C., Quinn, T. M., Lin, K., Taylor, F. W., et al. (2014). Persistent decadal-scale rainfall variability in the tropical South Pacific Convergence Zone through the past six centuries. *Climate of the Past 10*, 1319-1332. https://doi.org/10.5194/cp-10-1319-2014

McFarlin, J. M., Axford, Y., Masterson, A. L., & Osburn, M. R. (2019). Calibration of modern sedimentary $\delta^{2}H$ plant wax-water relationships in Greenland lakes. *Quaternary Science Reviews, 225*, 105978. https://doi.org/10.1016/j.quascirev.2019.105978

Meyers, P. A. (2003). Applications of organic geochemistry to paleolimnological reconstructions: a summary of examples from the Laurentian Great Lakes. *Organic Geochemistry, 34*(2), 261-289. https://doi.org/10.1016/S0146-6380(02)00168-7

Moore, P. D., Webb, J. A., & Collinson, M. E. (1991). Pollen analysis. Blackwell Scientific, Oxford.

Mueller-Dombois, D., & Fosberg, F. R. (1998). Vegetation of the tropical Pacific islands. Springer, New York.

Nelson, D. B., (2013). Hydrogen isotopes from lipid biomarkers: Purification, field calibration, and application to reconstructing Galapagos paleohyrology. University of Washington.

Nelson D. B., & Sachs J. P. (2016). Galápagos hydroclimate of the Common Era from paired microalgal and mangrove biomarker $^{2}H/^{1}H$ values. *Proceedings of the National Academy of Sciences of the United States of America, 113*(13), 3476-3481. https://doi.org/10.1073/pnas.1516271113

Nelson, D. B., Knohl, A., Sachse, D., Schefuß, E., & Kahmen, A. (2017). Sources and abundances of leaf waxes in aerosols in central Europe. *Geochimica et Cosmochimica Acta, 198*, 299-314. https://doi.org/10.1016/j.gca.2016.11.018

Nelson, D. B., Ladd, S. N., Schubert, C. J., & Kahmen, A. (2018). Rapid atmospheric transport and large-scale deposition of recently synthesized plant waxes. *Geochimica et Cosmochimica Acta, 222*, 599-617. https://doi.org/10.1016/j.gca.2017.11.018

Newberry, S. L., Kahmen, A., Dennis, P., & Grant, A. (2015). *n*-Alkane biosynthetic hydrogen isotope fractionation is not constant throughout the growing season in the riparian tree

Salix viminalis. *Geochimica et Cosmochimica Acta, 165*, 75-85. https://doi.org/10.1016/j.gca.2015.05.001

Osburn, M. R., Sessions, A. L., Pepe-Ranney, C., Spear, J. R. (2011). Hydrogen-isotopic variability in fatty acids from Yellowstone National Park hot spring microbial communities. *Geochimica et Cosmochimica Acta, 75*(17), 4830-4845. https://doi.org/10.1016/j.gca.2011.05.038

Partin, J. W., Quinn, T. M., Shen, C. -C., Emile-Geay, J., Taylor, F. W., Maupin, C. R., et al. (2013). Multidecadal rainfall variability in South Pacific Convergence Zone as revealed by stalagmite geochemistry. *Geology, 41*(11), 1143-1146. https://doi.org/10.1130/G34718.1

Peterse, F., van der Meer, M. T. J., Schouten, S., Jia, G., Ossebaar, J., Blokker, J., & Sinninghe Damste, J. S. (2009). Assessment of soil *n*-alkane δD and branched tetraether membrane lipid distributions as tools for paleoelevation reconstruction. *Biogeosciences, 6*, 2799-2807.

Prebble, M., & Wilmshurst, J.M. (2009). Detecting the initial impact of humans and introduced species on island environments in Remote Oceania using palaeoecology. *Biological Invasions, 11*, 1529–1556. https://doi.org/10.1007/s10530-008-9405-0

Prebble, M., Anderson, A. J., Augustinus, P., Emmitt, J., Fallon, S. J., Furey, L. L., et al. (2019). Early tropical Pacific production in marginal subtropical and temperate Polynesia. *Proceedings of the National Academy of Sciences of the United States of America 116*(18), 8824-8833. https://doi.org/10.1073/pnas.1821732116

Polissar, P. J., & Freeman, K. H. (2010). Effects of aridity and vegetation on plant-wax δD in modern lake sediments. *Geochimica et Cosmochimica Acta, 74*(20), 5785-5797. https://doi.org/10.1016/j.gca.2010.06.018

Quinn, T. M., Crowley, T. J., Taylor, F. W., & Henin, C. (1998). A multicentury stable isotope record from a New Caledonia coral: interannual and decadal sea surface temperature variability in the Southwest Pacific since 1657 AD. *Paleoceanography, 13*(4), 412-426. https://doi.org/10.1029/98PA00401

Quinn, T. M., Taylor, F. W., & Crowley, T. J. (1993). A 173 year stable isotope record from a tropical South Pacific coral. *Quaternary Science Reviews, 12*(6), 407-418. https://doi.org/10.1016/S0277-3791(05)80005-8

Reef R., Markham H. L., Santini N. S., & Lovelock C. E., (2015). The response of the mangrove *Avicennia marina* to heterogeneous salinity measured using a split-root approach. *Plant Soil, 393*, 297–305. https://doi.org/ 10.1007/s11104-015-2489-2

Richey, J. N., & Sachs, J. P. (2016). Precipitation changes in the western tropical Pacific over the past millennium. *Geology, 44*(8), 671-674. https://doi.org/10.1130/G37822.1

Rozanski, K., Araguas-Araguas, L, & Gonfiantinin, R. (1993). Isotopic patterns in modern global precipitation. In P. K. Swart (Ed.) *Climate Change in Continental Isotopic Records, Volume 78* (pp. 1-36). Washington, DC: American Geophysical Union. https://doi.org/10.1029/GM078p0001

Sachs, J. P., Blois, J. L., McGee, T., Wolhowe, M., Haberle, S., Clark, G., Atahan, P. (2018). Southward shift of the Pacific ITCZ during the Holocene. *Paleoceanography and Paleoclimatology, 33*(12), 1383-1395. https://doi.org/10.1029/2018PA003469

Sachs J. P., Sachse D., Smittenberg R. H., Zhang Z., Battisti D. S., & Golubic S. (2009). Southward movement of the Pacific intertropical convergence zone AD 1400–1850. *Nature Geoscience, 2*, 519–525. https://doi.org/10.1038/NGEO554

Sachse, D., Billault, I., Bowen, G. J., Chikaraishi, Y., Dawson, T. E., Feakins, S. J., et al. (2012). Molecular Paleohydrology: Interpreting the hydrogen-isotopic composition of lipid

biomarkers from photosynthesizing organisms. *Annual Review of Earth and Planetary Sciences, 40*, 221–249. https://doi.org/10.1146/annurev-earth-042711-105535

Sachse D., Radke J., & Gleixner G. (2004). Hydrogen isotope ratios of recent lacustrine sedimentary n-alkanes record modern climate variability. *Geochimica et Cosmochimica Acta, 68*(23), 4877-4889. https://doi.org/10.1016/j.gca.2004.06.004

Santini N. S., Reef R., Lockington D. A., & Lovelock C. E. (2015). The use of fresh and saline water sources by the mangrove Avicennia marina. *Hydrobiologia, 745*, 59–68. https://doi.org/10.1007/s10750-014-2091-2

Schwab, V. F., Garcin, Y., Sachse, D., Todou, G., Sene, O., Onana, J. M., et al. (2015). Effect of aridity on $\delta^{13}C$ and δD values of C3 plant- and C4 graminoid-derived leaf wax lipids from soils along an environmental gradient in Cameroon (Western Central Africa). *Organic Geochemistry, 78*, 99-109. https://doi.org/10.1016/j.orggeochem.2014.09.007

Sear, D. A., Allen, M. S., Hassall, J. D., Maloney, A. E., Langdon, P. G., Morrison, A. E., et al. (2020). Human settlement of East Polynesia earlier, incremental, and coincident with prolonged South Pacific drought. *Proceedings of the National Academy of Sciences of the United States of America, 117*(16), 8813-8819. https://doi.org/10.1073/pnas.1920975117.

Shanahan, T. M., Hughen, K. A., Ampel, L., Sauer, P. E., Fornace, K. (2013). Environmental controls on the $^{2}H/^{1}H$ values of terrestrial leaf waxes in the eastern Canadian Arctic. *Geochimica et Cosmochimica Acta, 119*, 286-301. https://doi.org/10.1016/j.gca.2013.05.032

Sharmila, S., & Walsh, K. J. E. (2018). Recent poleward shift of tropical cyclone formation linked to Hadley cell expansion. *Nature Climate Change, 8*, 730-736. https://doi.org/10.1038/s41558-018-0227-5

Sichrowsky, U., Schabetsberger, R., Sonntag, B., Stoyneva, M., Maloney, A. E., Nelson, D. B., et al. (2014). Limnological characterization of volcanic crater lakes on Uvea Island (Wallis and Futuna, South Pacific). *Pacific Science, 68*(3), 333-343. https://doi.org/10.2984/68.3.3

Smittenberg R. H., Saenger C., Dawson M. N., & Sachs J. P. (2011). Compound-specific D/H ratios of the marine lakes of Palau as proxies for West Pacific Warm Pool hydrologic variability. *Quaternary Science Reviews, 30*(7-8), 921-933. https://doi.org/10.1016/j.quascirev.2011.01.012

Southern, W. (1986). The Late Quaternary Environmental History of Fiji. Australian National University.

Steen-Larsen, H. C., Risi, C., Werner, M., Yoshimura, K., Masson-Delmotte, V. (2017). Evaluating the skills of isotope-enabled general circulation models against in situ atmospheric water vapor isotope observations. *JGR Atmospheres, 122*(1), 246-263. https://doi.org/10.1002/2016JD025443

Stevenson, J., Dodson, J. R., & Prosser, I. P. (2001). A late Quaternary record of environmental change and human impact from New Caledonia. *Palaeogeography, Palaeoclimatology, Palaeoecology, 168*(1-2), 97–123. https://doi.org/10.1016/S0031-0182(00)00251-0

Sturm, C., Zhang, Q., & Noone, D. (2010). An introduction to stable water isotopes in climate models: Benefits of forward proxy modeling for paleoclimatology. *Climate of the Past, 6*, 115-129. https://doi.org/10.5194/cpd-5-1697-2009

Tan, J., Jakob, C., Rossow, W. B., & Tselioudis, G. (2015). Increases in tropical rainfall driven by changes in frequency of organized deep convection. *Nature. 519*, 451-454. https://doi.org/10.1038/nature14339

Terry, J. P. (2011). The Climate of Santo (Vanuatu). In P. Bouchet, H. Le Guyander, O. Pascal (Eds.), *The Natural History of Santo* (pp. 52-56). Paris, France: Museum National d'Histoire Naturelle.

Tierney, J. E., deMenocal, P. B., & Zander, P. D. (2017). A climatic context for the out-of-Africa migration. *Geology*, 45 (11): 1023–1026. https://doi.org/10.1130/G39457.1

Tipple B. J., Berke M. A., Doman C. E., Khachaturyan S., & Ehleringer J. R. (2013). Leaf *n*-alkanes record the plant-water environment at leaf flush. *Proceedings of the National Academy of Sciences of the United States of America 110*(7), 2659–2664. https://doi.org/10.1073/pnas.1213875110

Tipple, B. J., Berke M. A., Hambach B., Roden J. S., & Ehleringer J. R. (2015). Predicting leaf wax *n*-alkane $^{2}H/^{1}H$ ratios: Controlled water source and humidity experiments with hydroponically grown trees confirm predictions of Craig-Gordon model. *Plant, Cell and Environment, 38*(6), 1035-1047. https://doi.org/10.1111/pce.12457

van Bree, L. G. J., Peterse, F., van der Meer, M. T. J., Middelburg, J. J., Negash, A. M. D., De Crop, W., et al. (2018). Seasonal variability in the abundance and stable carbon-isotopic composition of lipid biomarkers in suspended particulate matter from a stratified equatiorial lake (Lake Chala, Kenya/Tanzania): Implications for the sedimentary record. *Quaternary Science Reviews, 192*, 208-224. https://doi.org/10.1016/j.quascirev.2018.05.023

Volkman J. K. (2003). Sterols in microorganisms. *Applied Microbiology and Biotechnology, 60*, 495–506. https://doi.org/10.1007/s00253-002-1172-8

Volkman J. K., Johns R. B., Gillian, F. T., & Perry G. J. (1980). Microbial lipids of an intertidal sediment – I. Fatty acids and hydrocarbons. *Geochimica et Cosmochimica Acta, 44*(8), 1133-1143. https://doi.org/10.1016/0016-7037(80)90067-8

Wang, C., Hren, M. T., Hike, G. D., Zeng, J. L., & Garzione, C. N. (2017). Soil *n*-alkane δD and glycerol dialkyl glycerol tetraether (GDGT) distributions along an altitudinal transect from southwest China: evaluating organic molecular proxies for paleoclimate and paleoelevation. *Organic Geochemistry, 107*, 21-32. https://doi.org/10.1016/j.orggeochem.2017.01.006

Wu, M. S., West, A. J., & Feakins, S. J. (2019). Tropical soil profiles reveal the fate of plant wax biomarkers during soil storage. *Organic Geochemistry, 128*, 1-15. https://doi.org/10.1016/j.orggeochem.2018.12.011

Yoshimura, K., Kanamitsu, M., Noone, D., & Oki, T. (2018). Historical isotope simulation using reanalysis atmospheric data. *Journal of Geophysical Research: Atmospheres*, *113*(D19), D19108. https://doi.org/10.1029/2008JD010074

Zhang X., Gillespie A., & Sessions A. L. (2009). Large D/H variations in bacterial lipids reflect central metabolic pathways. *Proceedings of the National Academy of Sciences of the United States of America, 106*(31), 12580-12586. https://doi.org/10.1073/pnas.0903030106

Zhang Z., & Sachs J. P. (2007). Hydrogen isotope fractionation in freshwater algae: 1. Variations among lipids and species. *Organic Geochemistry, 38*(4), 582–608. https://doi.org/10.1016/j.orggeochem.2006.12.004

Table 1 Lake location, total number of core tops analyzed per site, δ^2H values of local precipitation and core top leaf waxes, and predicted δ^2H_{Wax} values based on relationships from literature compilation

Site, Island, Country	Lat. (°N)[1]	Long. (°E)[1]	# of core tops	δ^2H_P (‰, VSMOW)[2]	δ^2H *n*-C_{29} alkane (residual from global relationship) (‰, VSMOW)[3]	δ^2H *n*-C_{28} acid (residual from global relationship) (‰, VSMOW)[3]
Lakes						
Rimatu'u Pond, Tetiaroa, French Polynesia	−17.0249	210.4417	2	−25 ± 26	−177 (37)	−160 ± 17 (27)
Oroatera Pond, Tetiaroa, French Polynesia	−16.9958	210.4591	1	−25 ± 26	−173 (34)	*N.A.*
Onetahi Pond, Tetiaroa, French Polynesia[#]	−17.0207	210.4081	1	−25 ± 26	−139 (-1)	−126 (-6)
Lake Lanoto'o, Upolu, Samoa	−13.9109	188.1726	3	−34 ± 3	−159 (11)	−148 ± 6 (9)
Lac Lalolalo, Wallis, Wallis and Futuna	−13.3017	183.7662	3	−23 ± 1	*N.A.*	−150 ± 6 (19)
Lac Lanutavake, Wallis, Wallis and Futuna	−13.3212	183.7860	2	−24 ± 2	*N.A.*	−140 ± 9 (8)
Lake Dranoniveilomo, Vanua Balavu, Fiji	−17.1976	181.0441	2	−21 ± 11	−151 (14)	−173 ± 14 (43)
Lake Tagamaucia, Teveuni, Fiji[#]	−16.8163	180.0601	2	−34 ± 14	−170 ± 1 (22)	−175 ± 1 (36)
Otas Lake, Efate, Vanuatu	−17.6945	168.5850	1	−34 ± 73	−154 (6)	−136 (-3)
Emaotul Lake, Efate, Vanuatu	−17.7342	168.4151	3	−36 ± 76	−152 ± 9 (2)	−130 ± 3 (-10)
White Lake, Thion, Vanuatu	−15.0410	167.0892	2	−35 ± 70	−174 (25)	−119 ± 2 (-21)
Waérowa East Lake, Espiritu Santo, Vanuatu[#]	−15.5950	167.0788	1	−34 ± 71	*N.A.*	−155 (16)
Nopovois Pond, Espiritu Santo, Vanuatu	−15.4970	166.7357	1	−40 ± 71	−154 (0)	−122 (-22)
Vesalea Pond, Espiritu Santo, Vanuatu[#]	−15.1589	166.6549	1	−40 ± 70	−157 (3)	*N.A.*
Lake Hut, Grande Terre, New Caledonia	−22.2609	166.9526	2	−15 ± 54	−161 ± 2 (30)	−133 ± 1 (8)
Lake Tavara, Tetepare, Solomon Islands	−8.7029	157.4503	1	−46 ± 43	−162 (3)	−156 (8)
Lake Rano, Rendova, Solomon Islands	−8.6879	157.3243	2	−47 ± 42	*N.A.*	−135 ± 5 (-13)
Harai Lake #1, Rendova, Solomon Islands	−8.5622	157.3556	1	−47 ± 42	*N.A.*	−121 (-28)
Harai Lake #3, Rendova, Solomon Islands	−8.5648	157.3651	2	−47 ± 42	*N.A.*	−134 ± 11 (-16)
Mangrove swamps						
Sapwalap Swamp, Pohnpei, Fed. States of Micronesia	6.88	158.30	5	−33 ± 2	−150 ± 5 (2)	*N.M.*
Tol Swamp, Chuuk, Fed. States of Micronesia	7.35	150.60	4	−32± 1	−153 ± 5 (1)	*N.M.*
Sasa Swamp, Guam, United States	13.45	140.73	4	−29 ± 1	−145 ± 5 (6)	*N.M.*
Galal Swamp, Yap, Fed. States of Micronesia	9.50	138.08	5	−34 ± 1	−151 ± 6 (2)	*N.M.*

[1]Less precision is provided for latitude and longitude in mangrove swamps because swamp samples were collected along a transect typically spanning > 1 km.
[2]Mean annual precipitation δ^2H values (relative to VSMOW) from OIPC ± 95% confidence intervals.
[3]Mean value of multiple surface sediment measurements from same lake, relative to VSMOW. Uncertainties represent 1 standard deviation. When only one core top was analyzed no uncertainty is reported. Analytical uncertainty for compound specific δ^2H measurements is 4‰. *"N.A."* = compound was not present or was below detection limit for δ^2H measurements. "*N.M.*" = not measured. [#]Lakes with greater than 50% vegetation cover

1050 **Table 2** Regression statistics for linear relationships shown in Fig. 2, reported for the global data set with
1051 and without the new data points from the western tropical Pacific region. Uncertainties for slopes and y-
1052 intercepts represent standard errors.
1053

	Slope	y-intercept	R^2	*p*	n
n-C_{29}-alkane (all data)	0.93 ± 0.02	−117 ± 2	0.73	<0.0001	581
n-C_{29}-alkane (without WP)	0.94 ± 0.02	−116 ± 2	0.73	<0.0001	564
n-C_{29}-alkane (West Pacific)	−0.06 ± 3	−160 ± 15	0.02	0.98	17
n-C_{28}-acid (all data)	0.73 ± 0.03	−114 ± 3	0.74	<0.0001	242
n-C_{28}-acid (without WP)	0.74 ± 0.03	−113 ± 3	0.73	<0.0001	225
n-C_{28}-acid (West Pacific)	1.2 ± 3	−149 ± 17	0.01	0.69	17

Table 3 Pollen counts from near surface sediments, reported as a percentage of total palynmorphs counted. For each sediment sample, age ranges are presented for the top and bottom depth.

Site, Island, Country	Depth of pollen sample (cm)	Bacon age at top of interval (year C.E.)[$]	Bacon age at bottom of interval (year C.E.)[$]	Primary forest (%)	Secondary forest (%)	Mangroves (%)	Ferns (%)	Non-vascular plants (%)	Dryland herbs (%)	Wetland herbs (%)	Aquatic plants (%)	Unknown (%)
Lake Lanoto'o, Upolu, Samoa	1-2	2013 ± 1	2002 ± 1	3.0	24.6	0	62.8	0	2.7	6.9	0	0
Lac Lalolalo, Wallis, Wallis and Futuna*	1-3	2001 +8 -14	1991 + 14 -19	10.3	57.1	0	16.4	0	0.4	13.4	0.8	1.7
Lac Lanutavake, Wallis, Wallis and Futuna	3-4	1990 +20 -64	1983 +26 -86	13.1	69.1	0	4.3	0	6.2	4.6	0	2.7
Lake Dranoniveilomo, Vanua Balavu, Fiji	2-3	2010 ± 2	2009 ± 3	21.0	33.6	0.7	17.5	1.4	4.2	19.6	0	2.1
Lake Tagamaucia, Teveuni, Fiji[#]	2-3	1989 ± 7	1978 ± 10	5.1	13.4	0	58.6	0	0.6	21.3	0	1.0
Otas Lake, Efate, Vanuatu	2-3	N.A.	N.A.	4.7	52.1	15.6	2.7	0	0	21.8	0.8	2.3
Emaotul Lake, Efate, Vanuatu	1-2	2016 ± 3.4	2014 ± 3.4	4.9	55.8	0	12.7	0.3	11.4	8.4	5.2	1.3
White Lake, Thion, Vanuatu	3-4	1997 +23 -14	1991 +30 -19	1.3	42.3	0	39.3	0	2.1	11.7	0	3.4
Waérowa East Lake, Espiritu Santo, Vanuatu[#]	3-1	2010 ± 3	2009 ± 3	1.2	11.2	14.1	35.9	0	11.2	14.7	7.7	4.1
Nopovois Pond, Espiritu Santo, Vanuatu	0-1	2017	N.A.	16.3	53.5	0	15.0	0	8.9	3.1	0.3	2.6
Vesalea Pond, Espiritu Santo, Vanuatu[#]	0-1	2016 +1 -3	2005 +10 -14	6.5	46.2	0	18.8	1.5	11.4	6.8	4.6	4.3
Lac Hut, Grand Terre, New Caledonia	0-1	N.A.	N.A.	50.1	41.1	0	4.8	0	0	0.9	0	3.1
Lake Tavara, Tetepare, Solomon Islands	8-9	1996 ± 5	1993 ± 6	6.3	23.4	6.3	54.7	0	1.6	7.8	0	0.1
Lake Rano, Rendova, Solomon Islands	9-10	1969 +17 -16	1960 +21 -20	16.7	46.5	0	29.8	0	0	4.4	0.9	1.8
Harai Lake #1, Rendova, Solomon Islands	11-12	1716 +99 -123	1702 +103 -120	5.4	19.4	2.2	66.7	0	0	5.4	0	1.1
Harai Lake #3, Rendova, Solomon Islands	30-31	1871 ± 85	1866 +86 -84	3.1	5.2	0	91.8	0	0	0	0	0

*Mean of 2 samples from different sites in these lakes. Age ranges presented represented the mean age for the top and bottom of each interval, and the full range of possible ages for both sites.

Lakes with greater than 50% vegetation cover

$ Age ranges are provided from sites with existing age models, the details of which are provided by Maloney et al. (2019), Krentscher et al. (2019), Gosling et al. (2020), and Sear et al. (2020)